Knockout of cyclin dependent kinases 8 and 19 leads to depletion of cyclin C and suppresses spermatogenesis and male fertility in mice

Alexandra V. Bruter[1,2]*, Ekaterina A. Varlamova[1,2]*, Nina I. Stavskaya[1], Zoia G. Antysheva[3], Vasily N. Manskikh[4,5], Anna V. Tvorogova[1], D. S. Korshunova[1], Alvina I. Khamidullina[1,6], Marina V. Utkina[7], Viktor P. Bogdanov[3], Alyona I. Nikiforova[5], Eugene A. Albert[3], Denis O. Maksimov[3], Jing Li[8], Mengqian Chen[8,9], Alexander A. Shtil[2,6], Igor B. Roninson[8], Vladislav A. Mogila[6,8], Yulia Y. Silaeva[6], Victor V. Tatarskiy[1,6].

[1]Center for Precision Genome Editing and Genetic Technologies for Biomedicine, Institute of Gene Biology, Russian Academy of Sciences, 34/5 Vavilov Street, 119334 Moscow, Russia

[2]Blokhin National Medical Research Center of Oncology, 24 Kashirskoye Shosse, 115522 Moscow, Russia.

[3]Life Sciences Research Center, Moscow Institute of Physics and Technology, Dolgoprudniy, Russia.

[4]Belozersky Institute of Physico-Chemical Biology, Lomonosov Moscow State University, 119992 Moscow, Russia.

[5]Institute of Mitoengineering MSU, 119992 Moscow, Russia

[6]Institute of Gene Biology, Russian Academy of Sciences, 34/5 Vavilov Street, 119334 Moscow, Russia

[7] Endocrinology Research Centre, 117292 Moscow, Russia

[8]Department of Drug Discovery and Biomedical Sciences, University of South Carolina, 715 Sumter Street, Columbia, SC 29208, USA

[9]Senex Biotechnology, Inc., 715 Sumter Street, Columbia, SC 29208, USA

*These authors contributed equally to this work

Abstract

CDK8 and CDK19 are regulatory kinases associated with the transcriptional Mediator complex. We have generated mice with the systemic deletion of both *Cdk19* (constitutive knockout) and *Cdk8* (inducible knockout). *Cdk8/19* double knockout (DKO), in contrast to the deletion of *Cdk8* or *Cdk19* alone or treatment with a CDK8/19 kinase inhibitor, led to depletion of cyclin C (CcnC), the binding partner of CDK8/19 that has been implicated in CDK8/19-independent functions. DKO males were infertile. The DKO males lacked postmeiotic spermatids and spermatocytes after meiosis I pachytene. Testosterone levels were decreased whereas the amounts of the luteinizing hormone were unchanged. Single cell RNA sequencing showed marked differences in the expression of steroidogenic genes (such as *Cyp17a1, Star* and *Fads*) in Leydig cells concomitant with alterations in Sertoli cells and spermatocytes likely associated with impaired synthesis of steroids. *Star* and *Fads* were also downregulated in cultivated Leydig cells after DKO. In contrast to DKO, the treatment of Leydig cells with a CDK8/19 inhibitor did not induce the same changes in gene expression, prolonged treatment of mice with a CDK8/19 inhibitor did not affect the size of testis, suggesting that the observed phenotype was likely mediated through kinase-independent activities of CDK8/19, such as CcnC stabilization.

List of abbreviations

4-OHT – 4-hydroxytamoxifen

AR – androgen receptor

BTB – blood-testicular barrier

CcnC – Cyclin C

CKM – cyclin dependent kinase module

DEG – differentially expressed genes

DKO – double knockout

LH – luteinizing hormone

PI – propidium iodide

RNA Pol II – RNA polymerase II

scRNAseq – single cell RNA sequencing

SenB – Senexin B

TF – transcription factor

Introduction

Multiple protein complexes regulate transcription, in response to developmental cues, changes in environment, damage and other factors, allowing for precise control of gene expression. Among such complexes the multiprotein Mediator complex is especially important for controlling transcription, regulated by a multitude of signaling pathways through their transcription factors (TFs). The Mediator complex bridges the regulatory enhancer regions with promoters thereby recruiting RNA polymerase II (RNA Pol II) and the preinitiation complex. The Mediator possesses its own regulatory subpart – the cyclin dependent kinase module (CKM), containing either the CDK8 or the CDK19 protein kinases, in complex with their binding partner cyclin C (CcnC), as

well as proteins MED12 and MED13 (Luyties and Taatjes, 2022). While CKM is a nuclear complex that regulates transcription, both CcnC (Ježek et al. 2019) and MED12 (S. Zhang, O'Regan, and Xu 2020) were shown to have CKM-independent cytoplasmic activities. CDK8/19 kinase activity positively regulates transcription induced by different signals (Chen et al. 2017, Chen et al. 2023), at least in part by mediating the RNA Pol II release from pausing (Steinparzer et al. 2019). Besides, CDK8 and CDK19 directly phosphorylate a number of transcription factors such as STATs (Martinez-Fabregas et al. 2020), SMADs (Alarcón et al. 2009) and others, thereby modulating transcription of cognate genes. CDK8/19 kinase activity also negatively regulates transcription, at least, in part through downregulating the protein levels of all the components of the Mediator and CKM (Chen et al. 2023).

Despite important CDK8/19 functions discovered in primary cell culture and cell lines (Luyties and Taatjes, 2022), the insights gained from in vivo models are limited. Mice with constitutively knocked out *Cdk19* (CDK19 KO) were generated as a part of the COMP project and are basically asymptomatic, fertile, and have normal lifespan. It has been shown recently that *Cdk19*$^{-/-}$ Lin^{-} hematopoietic stem cells divide slower (Zhang et al. 2022), however the blood cell count was unaffected. Heterozygous mice with constitutive *Cdk8* knockout were asymptomatic but, when crossed, no homozygous pups were born (Postlmayr et al. 2020; Westerling et al. 2007). Moreover, conditional *Cdk8* KO is almost asymptomatic in adult mice, and the lifespan is normal. Minor differences were observed in colon epithelial differentiation (Dannappel et al. 2022; Prieto et al. 2023) and tumorigenesis (McCleland et al. 2015) as well as in osteoclastogenesis (Yamada et al. 2022) after tissue specific *Cdk8* knockout. Although two CDK8/19 inhibitors were reported to have systemic toxicity (Clarke et al. 2016), this toxicity was subsequently found to be due to off-target effects of these inhibitors (Chen et al. 2019), and several CDK8/19 inhibitors have

reached clinical trials (clinicaltrials.gov NCT03065010, NCT04021368, NCT05052255, NCT05300438). Several studies reported the existence of kinase-independent phenotypic activities for both CDK8 (Menzl et al. 2019; Kapoor et al. 2010) and CDK19 (Audetat et al. 2017; Steinparzer et al. 2019), but the only known biochemical activity of both Cdk8 and Cdk19 that is kinase-independent is the stabilization of their binding partner CcnC (Barette et al. 2001; Chen et al. 2023). Targeted degradation or knockout of both CDK8 and CDK19 dramatically reduces the cellular levels of CcnC, whereas the knockout of either *Cdk8* or *Cdk19* alone has little effect on CcnC levels (Chen et al. 2023). The effects of double knockout of both *Cdk8* and *Cdk19* on CcnC should therefore be considered in interpreting the effect of the double knockout.

We have for the first time generated mice with a conditional knockout of the *Cdk8* gene on the constitutive *Cdk19* KO background (CDK8/19 double knockout, DKO). We have found that CDK8/19 DKO males were completely infertile, had an undersized and dedifferentiated reproductive system. In CDK8/19 DKO males, spermatogenesis was completely blocked after pachytene of meiosis I. CDK8/19 DKO showed down-regulation of key steroid pathway genes, such as *Cyp17a1*, *Star* and *Lcn2*, *Sc5d*, *Fads2* and reduced production of testosterone. The Sertoli cells showed dysregulation of genes related to cytoskeleton and cell-cell contacts critical for their function. Finally, the expression of key meiotic genes was deregulated in meiosis I pre-diplotene spermatocytes, subsequently the progression of meiosis was halted. These results indicated a key role of CDK8/19-CcnC complex in the maintenance of male reproductive system.

Results

Cdk8/19 DKO leads to the loss of Cyclin C

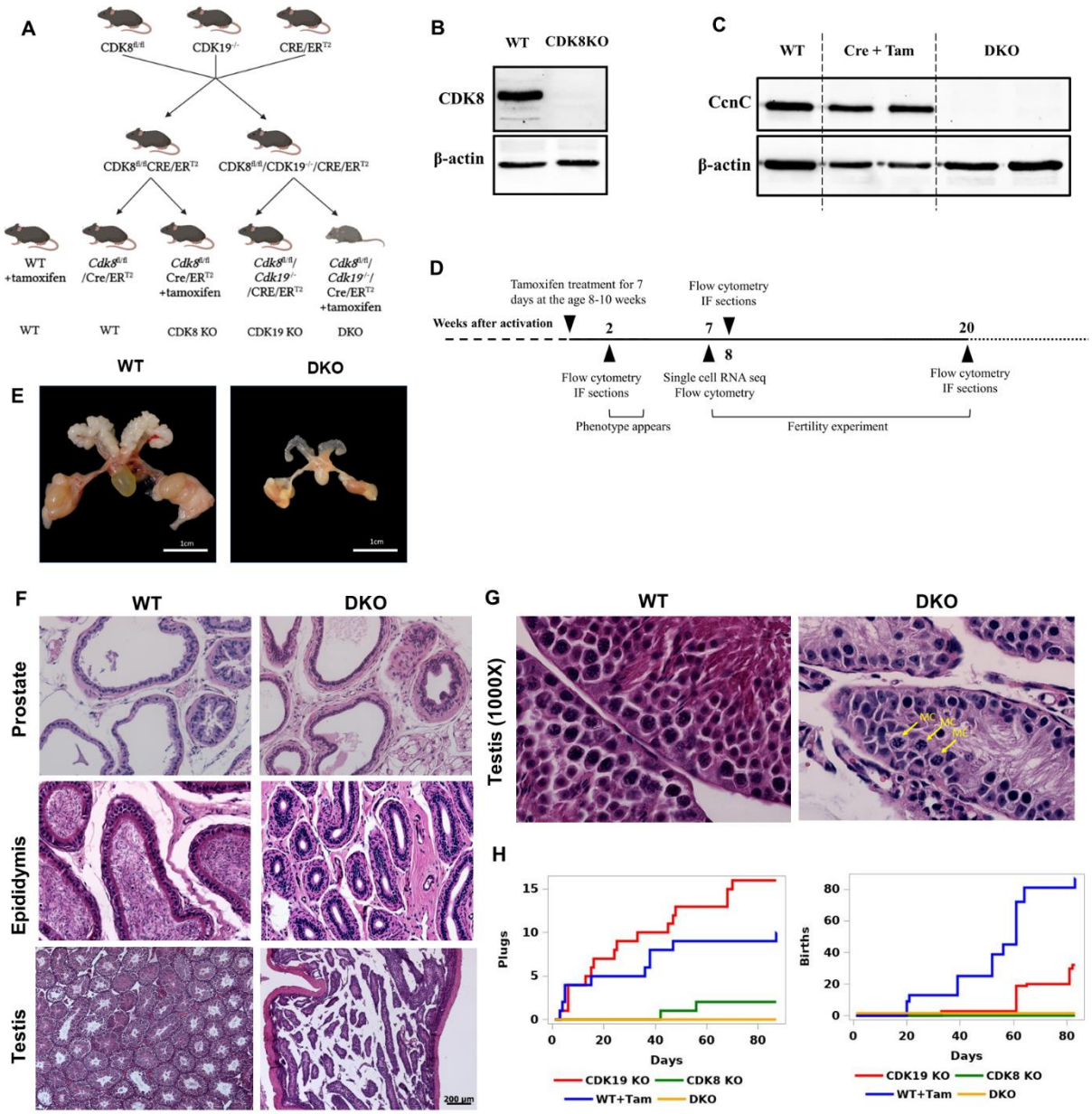

Figure 1. *Cdk8/19* knockout blocks spermatogenesis in mice. *(A)* Crossing of *Cdk8*$^{fl/fl}$, *Cdk19*$^{-/-}$ and *Cre/ER*^{T2} mice and formation of experimental (*Cdk8*$^{fl/fl}$*Cdk19*$^{-/-}$*Cre/ER*^{T2} + tamoxifen,

Cdk8$^{fl/fl}$Cre/ER^{T2} + tamoxifen and *Cdk19*$^{-/-}$) and control (*Cdk8*$^{fl/fl}$*Cdk19*$^{-/-}$*Cre/ER*^{T2} without tamoxifen and wild-type + tamoxifen) groups. *(B)* Confirmation of tamoxifen-induced CDK8 KO in testis by Western blot. *(C)* Cyclin C protein is absent in DKO, but not single KO in the testes. *(D)* Time course of experiments. CDK8 KO was activated by tamoxifen administration in males of 8-10 weeks old. Urogenital abnormalities became visible in two weeks. Spermatogenesis was analyzed by flow cytometry and immunofluorescence (IF) after 2, 8 and 20 weeks since activation. Single cell RNA sequencing was performed after 7 weeks of KO. *(E)* Male urogenital system atrophy in DKO mice. *(F)* H&E staining of prostate, epididymis and testis of DKO mice and tamoxifen-treated control. Impaired secretory function of prostate, empty epididymal ducts and lack of postmeiotic cells in DKO. 100X magnification *(G)* H&E staining of WT and DKO seminiferous tubules. Yellow arrows indicate colchicine-like figures in the nuclei of dying cells.1000X magnification. *(H)* Sexual behavior and fertility of tamoxifen treated, single KOs and DKO male mice.

Previously we have crossed *Cdk8*$^{fl/fl}$ mice with Rosa-Cre/ER^{T2} with tamoxifen-inducible Cre activity (Ilchuk et al. 2022) (Fig. 1A). Mice after tamoxifen activation at the age of 2 months were viable, had normal lifespan and showed no visible abnormalities, in agreement with the previous report (McCleland et al. 2015). However, even with enhanced activation scheme (3 mg of tamoxifen daily for 7 days) we were unable to achieve complete CDK8 KO in the brain, uterus and ovary. Inactivation of the gene in the testis was efficient at the protein and DNA levels (Fig. 1B, Supplementary Figure S1A). To investigate the effects of the double knockout of *Cdk8* and *Cdk19*, we crossed *Cdk8*$^{fl/fl}$*/Rosa-Cre/ER*^{T2} mice with *Cdk19*$^{-/-}$ mice generated in the Jackson Laboratory and bred at our facility. Single CDK19 KO mice were viable and fertile and were

maintained as homozygotes. We injected tamoxifen into 2 months old *Cdk8*$^{fl/fl}$*/Cdk19*$^{-/-}$*/Rosa-Cre/ER*^{T2} male and female mice. Age matched tamoxifen-treated wild-type mice served as a control. The DKO mice were viable and subsequently analyzed in necropsies.

We have analyzed the levels of the CDK8/19 binding partner CcnC after CDK8 KO, CDK19 KO and DKO in mouse embryonic fibroblasts and in mouse testes after DKO. In agreement with previous observations in human cell lines (Chen et al. 2023), CcnC was undetectable in DKO embryo fibroblasts as well as in DKO testes, but not in single CDK19 KO (Supplemental Fig. S1B, Fig. 1C). Hence, the protection of CcnC from proteolytic degradation by CDK8 and CDK19 occurs not only in human but also in mouse cells and tissues.

Spermatogenesis is blocked in CDK8/19 DKO males

To investigate CDK8/19 DKO effects we performed necropsy 8 weeks post tamoxifen (Fig. 1D) with subsequent H&E staining. The most striking results were observed in the urogenital system. The prostate, testicles and the epididymis were significantly smaller compared to single KO and tamoxifen-treated wild-type mice (Fig. 1E), the diameter of testicular tubules was diminished (Fig. 1F). The germinal epithelium of the tubules was presented by Sertoli cells with typical large light nuclei and some spermatogonia or spermatocytes. Cells at the next stages of spermatogenesis such as round spermatids and mature spermatids were completely absent. Among the spermatogenic cells there were early prophase cells but no other meiotic cells were observed. In contrast, we detected cells with a colchicine-like mitotic catastrophe and apoptotic bodies (Fig. 1F,G, yellow arrows). Thus, in this mouse the spermatogenesis progenitor cells were present but differentiation and/or meiosis was blocked. In Sertoli cells the vacuoles are the sign of the loss of contact between these cells and spermatogenic elements (Fig. 1F,G). Leydig cells were

significantly smaller and were almost depleted of secretory vacuoles suggesting the lack of hormonal activity. The epididymis contained empty (no sperm) tubules; the epithelium looked undifferentiated, that is, neither typical borders between epithelial cells nor clear Golgi zone were visible. The prostate and the epididymis were also atrophic (Fig. 1F). These changes were detectable from 2 weeks after tamoxifen treatment and persistent for at least 6 months (Fig. 1D). However, they were not observed in CDK8 KO and CDK19 KO (Supplemental Fig. S1C).

CDK8/19 DKO and CDK8 KO mice are infertile

To prove the infertility of CDK8/19 DKO mice we assessed sexual behavior and number of pups. As tamoxifen has an impact on the male reproductive system (Willems et al. 2011), we used tamoxifen-treated C57BL/6 mice as a control. The experiment was performed at least 6 weeks post injection. Four groups were enrolled in the experiment: tamoxifen treated C57BL/6 (WT+Tam), tamoxifen treated *Cdk8*$^{fl/fl}$*Rosa-Cre/ERT2* (CDK8 KO), *Cdk8*$^{fl/fl}$*Cdk19*$^{-/-}$*Rosa-Cre/ER*^{T2} (CDK19 KO) and tamoxifen treated *Cdk8*$^{fl/fl}$*Cdk19*$^{-/-}$*Rosa-Cre/ER*^{T2} (DKO). Three males in each group were kept separately with two outbred CD1 females for 3 months old. Copulative plugs and the number of pups were checked 5 days a week (Fig. 1H). Tamoxifen-treated wild-type mice demonstrated normal fertility: 10 plugs were detected and 86 pups were born. The CDK19 KO group showed slightly reduced fertility: 16 plugs but only 32 pups, probably because of a lower rate of pregnancy. Surprisingly, only two plugs and no pups were observed in the *Cdk8*$^{-/-}$ group despite normal appearance and behavior of males, and no microscopic abnormalities in seminiferous tubules (Supplemental Fig S1). Neither plugs nor pups were detectable in the CDK8/19 DKO cohort (Fig. 1H). These experiments showed that both CDK8 single KO and

CDK8/CDK19 DKO are infertile, and the cause of *Cdk8*$^{-/-}$ infertility is likely to be the lack of sexual behavior.

The 4n spermatocyte population is present in the testes of DKO mice while 1n spermatids are almost absent

H&E staining offers qualitative characterization of the spermatogenesis disorder. To obtain quantitative results we performed cell cycle analysis by flow cytometry with propidium iodide staining. In testicular cells, this method allows to distinguish between 4n primary spermatocytes that entered meiosis, 2n cells (Leidyg, Sertoli and other somatic cells, spermatogonia stem cells and secondary spermatocytes, that completed first meiotic division) and two 1n groups: round spermatids and elongated spermatids after DNA compaction as well as apoptotic (subG1) cells (Fig. 2A, *left*) (Pereira et al. 2016; Jeyaraj et al. 2003).

We examined the tissues of the wild-type *vs* single KO (either CDK8 KO or CDK19 KO) or DKO animals sacrificed two months after tamoxifen. Cell cycle analysis revealed striking differences in CDK8/19 DKO mice, with disappearance of elongated spermatids, and almost all round spermatids and massive cell death (Fig. 2A, *right*,B). The single CDK8 KO and CDK19 KO, as well as tamoxifen-treated wild-type controls, had the same cell distribution as tamoxifen-untreated wild-type mice (Fig. 2B). Noticeably, the 4n population and cells in the S-phase were not impaired by CDK8/19 DKO indicating that DKO spermatogonia successfully entered meiosis but could not produce haploid spermatids. This ongoing “meiotic catastrophe” led to almost full depopulation of the testis in DKO mice (Fig. 2C). Due to fast transition from meiosis I to meiosis

II it is difficult to detect secondary spermatocytes. Further investigation was aimed at identifying the time of meiotic cell death in DKO males.

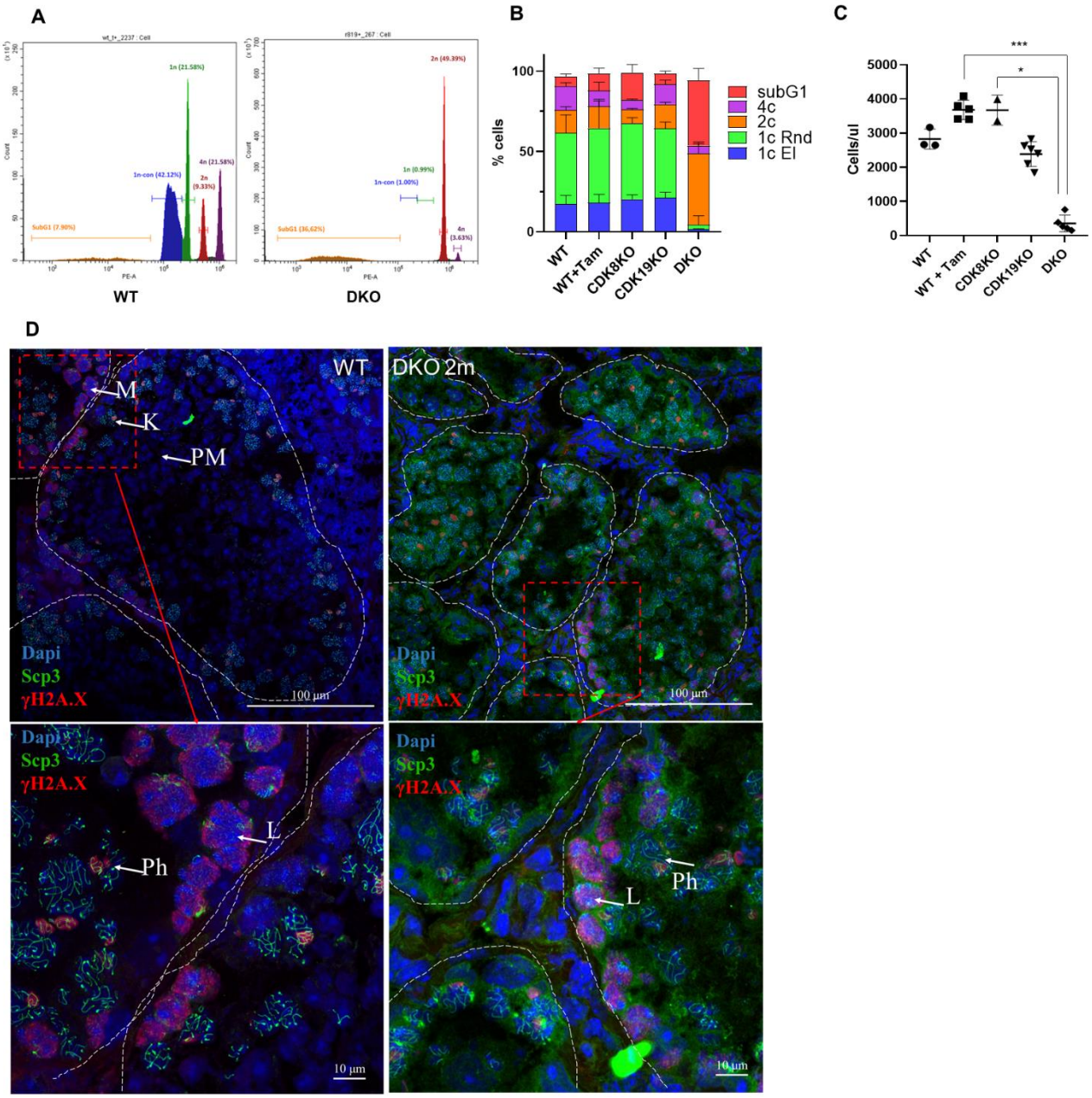

Figure 2. Absence of postmeiotic 1n cells in DKO 2 months after KO induction. *(A)* Distinctive histograms of wild-type (*left*) and DKO (*right*) mice. Violet - 4n population, red - 2n population, green - round spermatids, blue - elongated spermatids, orange - apoptotic subG1 cells. *(B)*

Quantitative distribution of testis cells between these groups. Wild type with and without tamoxifen as control groups have similar distribution to CDK8 and CDK19 single KO. DKO testes have greatly reduced number of round spermatids and no elongated spermatids. *(C)* Overall cellularity is also significantly reduced only in DKO testes. *(D)* IF staining of control and DKO testis frozen sections. Nuclei are stained by DAPI (blue pseudocolor), SYCP3 is depicted as green, γH2A.X - as red. All stages of spermatogenesis are visible in control testis, while pachytene is the last detected stage in DKO. Confocal microscopy, magnification 600X.

Spermatogenic cells of CDK 8/19 DKO mice are unable to advance through meiosis I prophase

To specify the time point of CDK8/19-dependent spermatogenesis failure we performed phospho-γH2A.X and SYCP3 immunohistochemical staining of seminiferous tubules of control tamoxifen-treated wild-type mice and DKO mice. The phosphorylated form of histone H2A.X is a DNA damage marker which becomes detectable after double-strand breaks formation in the leptotene, peaks in the zygotene and remains only in sex chromosomes during the pachytene. SYCP3 is a component of the synaptonemal complex required for crossover and homologous recombination. SYCP3 is expressed during meiosis I prophase and forms distinct patterns in the late zygotene/pachytene. In the wild-type tubules all the meiosis stages were visible (Fig. 2D). At the same time almost all meiotic cells in DKO were blocked in the pachytene (Fig. 2D), indicating that DKO cells enter meiosis but cannot traverse through meiosis I prophase and subsequently undergo cell death.

Single cell RNA sequencing

To investigate molecular mechanisms of CDK8/19 mediated alterations in meiosis we performed single cell RNA sequencing (scRNAseq) of the testis. This method allows one to identify all the cells in the groups (spermatogonia, different prophase stages, primary spermatocytes, secondary spermatocytes, round and elongated spermatogonia, Leydig cells, Sertoli cells, etc) based on their gene expression patterns and to trace differential gene expression in each group. We analyzed cell suspensions from testes of two tamoxifen-treated wild-type C57/BL/6 and two DKO animals. Similarly to flow cytometry experiments, knockouts were activated in two-months old mice and assayed two months after treatment with tamoxifen. The phenotype was confirmed by cell cycle analysis of a portion of cell suspension used for the 10X library preparation. Flow cytometry analysis showed complete absence of haploid cells in one DKO animal while the other had a subpopulation of round but not elongated spermatids (Supplemental Fig. S2).

The analysis of cell type composition confirmed the observed differences between wild-type and DKO animals. In agreement with flow cytometry and histological data the spermatids were almost completely absent in both DKO males and the number of spermatocytes at the stages post meiosis I prophase was greatly reduced (Fig. 3A,B). Clustering also confirmed the absence of cells after early pachytene while the meiotic entry, the leptotene and zygotene remained unaffected (Fig. 3B) confirming SYCP3 staining data. At the same time the percentage of undifferentiated spermatogonial stem cells in DKO animals was unchanged, nor was the proportion of Leydig cells altered. Sertoli cells were the only predominant cell type in DKO mice.

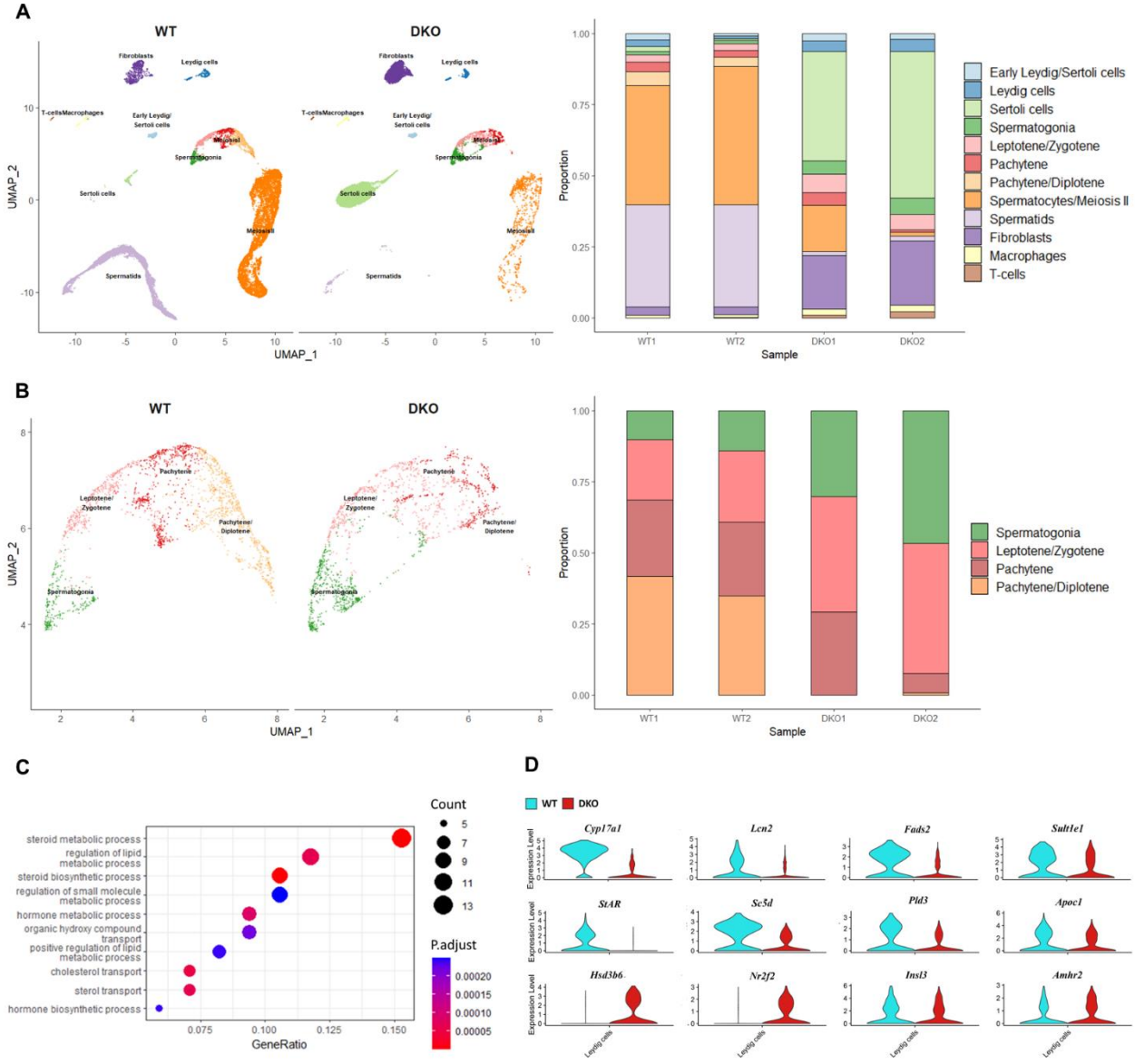

Figure 3. Single cell RNA sequencing reveals loss of spermatids due to steroidogenesis failure. *(A)* UMAP projection and relative cell numbers for all testis cell types in two control and two DKO samples. Number of secondary spermatocytes is significantly decreased and spermatids are almost absent in DKO samples. *(B)* UMAP projection and relative cell numbers for spermatogonia and primary spermatocytes. Post-pachytene spermatocytes are absent in DKO samples. *(C)* GO Biological Processes pathways enriched among Leydig cells differentially expressed genes

(DEGs). Lipid metabolism and steroid biosynthesis is severely perturbed. *(D)* Violin plots for key Leydig cell genes.

Differential gene expression

Differentiation of sperm lineage is a tightly controlled process, where changes in functioning in a certain type of cells can affect the viability and differentiation of other cells. To understand the underlying mechanism of meiotic cell death in DKOs we compared gene expression in each type of cell clusters present both in wild-type and knockout animals.

Leydig cells

Table 1. Down-regulated genes according to gene ontology (GO). List of differentially expressed genes with |log2FC|>1; p<0.01 their function in Leydig cells and reported phenotypes associated with infertility.

Gene	**Name**	**Log2FC**	**p.adjust <10^{-n}**	**Related fertility phenotype**	**Function**
Cyp17a1	Cytochrome P450 family 17 subfamily A member 1	-3.27	84	(Aherrahrou et al. 2020)	Enzyme in steroidogenic pathway
Hsd3b6	Hydroxy-delta-5-steroid dehydrogenase, 3 beta- and steroid delta-isomerase 6	1.18	11		
Lcn2	Lipocalin 2	-1.55	15		Transport small hydrophobic molecules such as lipids, steroid hormones and retinoids
Star	Steroidogenic Acute Regulatory Protein	-1.1	4		Cholesterol transporter
Apoc1	Apolipoprotein C1	-1.09	7		Inhibitor of cholesteryl ester transfer protein
Sc5d	Sterol-C5-Desaturase	-1.33	9		Desaturase
Fads2	Fatty acid desaturase 2	-1.26	19	(Stoffel et al. 2008)	
Sult1e1	Sulfotransferase Family 1E Member 1	-1.26	7	(Song 2007)	Androgen-dependent estrogen inactivation
Neat1	Nuclear Enriched Abundant Transcript 1	-1.04	17		Long non-coding RNA
Pld3	Phospholipase D Family Member 3	-1.04	11		Catalyze the hydrolysis of membrane phospholipids
Aqp5	Aquaporin 5	-1	5		Osmos
Klk1b27	Kallikrein 1-related peptidase b27	-2.52	15		Serine protease
Klk1	Kallikrein 1	1.7	13		
Serpina3g	Serpin Family A Member 3	1.08	32		

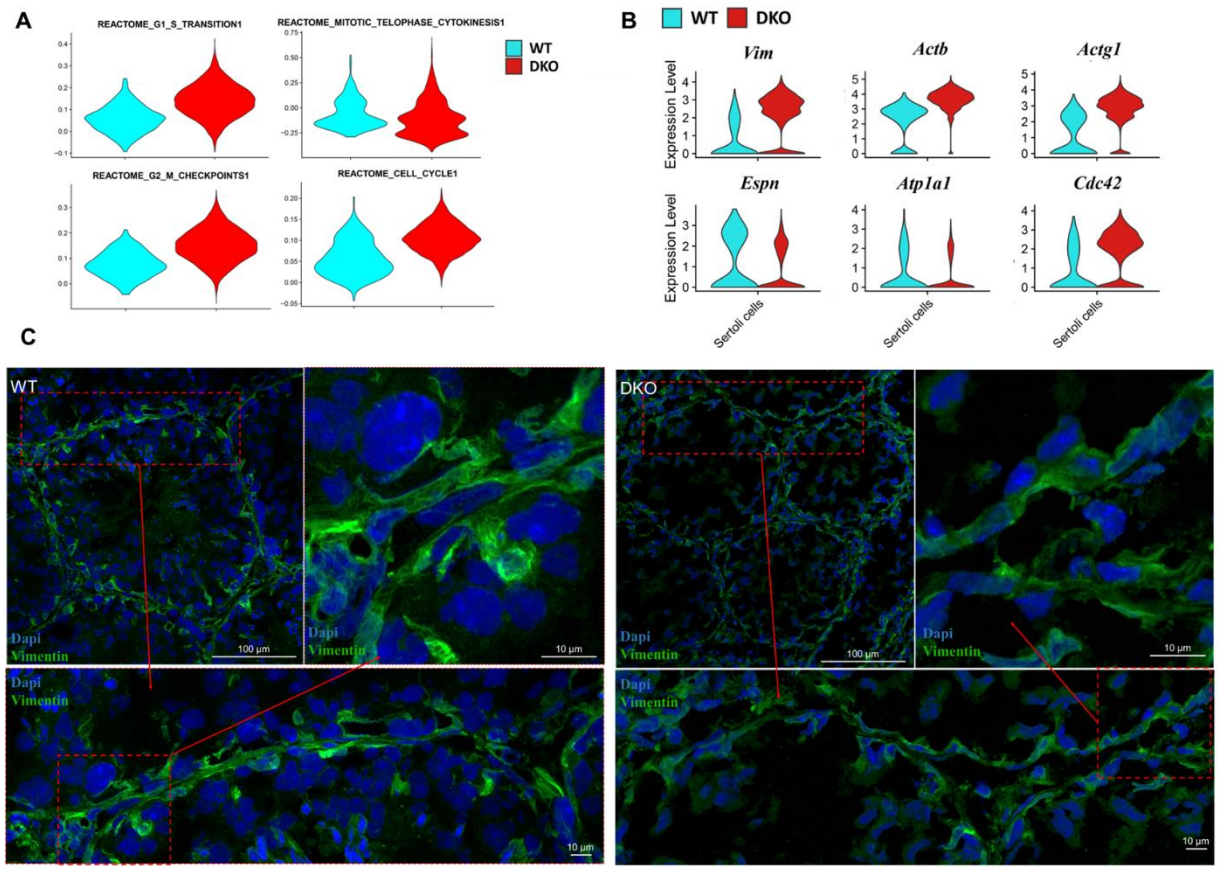

D

Description (ID)	GeneRatio	p.Adjust * 10^{-5}
response to oxidative stress (GO:0006979)	20/293	0,57
response to endoplasmic reticulum stress (GO:0034976)	16/293	0,57
cellular response to chemical stress (GO:0062197)	17/293	1,9

Figure 4. DKO Sertoli cells re-enter the cell cycle and lose characteristic cytoskeleton organization. *(A)* Violin plots for Reactome cell cycle gene sets indicate that Sertoli cells in DKO lose terminal differentiation and re-enter cell cycle. Fractions of cells in G1-S and G2-M transitions are increased in DKOs. *(B)* Violin plots for key cytoskeleton and intercellular contacts related DEGs. *(C)* IF staining for vimentin demonstrates blood-testicular barrier (BTB) integrity

disruption and loss of characteristic striation cytoskeleton patterns in DKOs. Magnification 600X. *(D)* Enrichment of GO stress pathways in Sertoli cells indicates their dysfunction in DKOs.

Leydig cells are the primary source for testosterone in the testis, a hormone required for spermatogenesis. scRNAseq analysis showed significant transcriptomic changes in Leydig cells. Among 126 genes that were differentially expressed ($|log2FC|>0.4$; $p<0.01$) in WT *vs* DKO Leydig cells, 30 were down-regulated, while among strongly affected genes with $|log_2FC|>1.11$ of 14 genes were down-regulated. Strikingly, 9 of 14 strongly downregulated genes were associated with to lipid (specifically steroid) metabolism (table 1) and 3 of these 9 genes were linked to male infertility.

According to the GO analysis (Fig. 3C, Supplemental table S1), the most prominent changes were downregulation of lipid metabolism and the steroid hormone biosynthesis. The most significantly down-regulated gene was *Cyp17a1*, showing 10-fold decrease (Fig. 3D). The *Cyp17a1* gene in males is mainly expressed in Leydig cells and, in contrast to humans, is silenced in adrenal glands (Missaghian et al. 2009). The product of this gene catalyzes the key reaction of the steroidogenic pathway. Mice with constitutive *Cyp17a1* KO were phenotypically female (Aherrahrou et al. 2020). Downregulated *Lcn2* (Fig. 3D) specifically expressed in Leydig cells codes for a protein of the lipocalin family that transports small hydrophobic molecules including steroids and is affected by fertility manipulations (Kang et al. 2017; Yanai et al. 2021). Another downregulated gene, *Fads2* (Fig. 3D), is a key enzyme for biosynthesis of highly unsaturated fatty acids. Its KO causes infertility in males by arresting the spermatogonial cycle at the stage of the round spermatid (Stroud et al. 2009). The *Sult1e1* (Fig. 3D) gene encodes sulfotransferase which inactivates estrogens and its deficiency leads to hyperplasia of Leydig cells and atrophy of

seminiferous tubules (Song 2007). The *Star, Sc5d, Pld3* and *Apoc1* (Fig. 3D) genes, involved in lipid metabolism, were down-regulated more than 2-fold. Interestingly, the *Hsd3b6* (Fig. 3D) is a surprisingly upregulated gene associated with steroid metabolism in Leydig cells.

Not only testosterone production was decreased in double knockouts. Expression of *Insl3* gene, coding for an important peptide hormone secreted by Leydig cells (Esteban-Lopez and Agoulnik 2020), was also reduced.

A more surprising group of genes affected by DKO are kallikreins (*Klk1b27, Klk1b21, Klk1, Klk1b24, Klk1b1, Klk1b8*) coding for serine peptidases (Supplemental table S2). This effect can be explained by steroid responsiveness of their locus (Lawrence et al. 2010). Their alterations have been reported in transcriptomic fertility studies (Behr et al. 2007; Dong et al. 2014), but, despite the growing evidence of their role in Leydig cells, the precise mechanism remains obscure.

Among up-regulated genes, several transcription factors governing steroidogenesis in Leydig cells were found (Ye et al. 2017; de Mattos et al. 2022). One of them, *Nr2f2* (Fig. 3D) encodes COUP-TFII which regulates genes immediately involved in steroidogenesis (*Cyp17a1, Hsd3b1, Cyp11a1* and *Akr1c14*) alongside several other Leydig-specific genes (*Insl3, Amhr2*) (Fig. 3D). Another gene, *Cebpb*, encodes TF C/EBPβ which activates Star transcription and stimulates expression of *Nr4a1* (also known as *Nur77*) which is itself a key regulator of steroidogenesis in Leydig cells.

The *Kit* gene (down-regulated), encoding a receptor with tyrosine kinase function, and Kitl gene (up-regulated), encoding its ligand, were also present among differentially expressed genes. Both of these genes play an important role in spermatogenesis (knockouts and mutants are infertile), Leydig cell maturation and steroidogenesis (Liu et al. 2017; Ye et al. 2017).

We hypothesize that the observed upregulation of several steroidogenesis regulators may be a part of a compensation feedback loop in response to the decreased testosterone level.

Sertoli cells

According to downregulation of the steroid hormone biosynthesis in Leydig cells we expected to see in Sertoli cells patterns similar to those in mice with Sertoli cell specific KOs of androgen receptor (AR) – SCARKO (Sertoli Cells Androgen Receptor KnockOut) (Larose et al. 2020; De Gendt et al. 2014) and luteinizing hormone (LH) receptor – LURKO (Griffin et al. 2010). However, it must be noted that these mice have constitutive receptor KOs and do not fully develop their reproductive system, whereas our KO model mice develop normally and become fertile before the knockout induction.

Single cell RNA sequencing (Fig. 3A, B) shows that Sertoli cell fraction is greatly increased in DKO specimens. Normally, Sertoli cells are terminally differentiated cells resting in the G0 phase of cell cycle. However, analysis of cell cycle-specific genes revealed that in DKO Sertoli cells can re-enter the cell cycle and proliferate (Fig. 4A). In particular, genes involved in G0-S transition and G2-M transition were upregulated. Thus, we suppose that the increase of Sertoli cell fraction is partially explained by their regained ability to proliferate due to the hormonal deficit. Another part of this increase is the reduction of absolute numbers of cells of other types.

The difference in Sertoli cell fractions makes differential gene expression analysis more complicated. However, among DEGs we identified a number of upregulated and downregulated genes consistent with their changes in SCARKO (*Defb45*, *Myl6*, *Tmsb4x*, *Espn*, *Ldhb* among top DEGs). We compared our DEG set with those published earlier (Larose et al. 2020; De Gendt et

al. 2014) and observed very little overlap between our data and published results as well as between the two published papers (Supplemental Fig. S3).

However, a much better agreement was found between our data and the study by deGendt et.al. (De Gendt et al. 2014) at the level of GO Molecular Function and Cellular Compartment categories.

According to the GO Cellular Compartment (Supplementary Table S1), both up- and down-regulated genes are associated with cytoskeleton, apical-basal axis, cellular membrane and intercellular contacts. These closely related structures play an important role in Sertoli cell functioning: formation of the blood-testicular barrier (BTB) and intercommunication with developing germ cells (Wong and Cheng 2009). Several of these genes have a described role in Sertoli cell morphology and functioning.

Vimentin, commonly used as a Sertoli cell marker, composes a Sertoli-specific intermediate filament, which polymerizes in an androgen-dependent manner (Show et al. 2003). Expression of the *Vim* gene was upregulated ~ 2-fold , as well as the actin genes *Actb* and *Actg1* (Fig. 4B). Expression of down-regulated *Espn* (Fig. 4B) gene coding actin-binding protein espin present in basal and apical ectoplasmic specialization was also significantly affected in SCARKO (Willems et al. 2010). Moreover, its localization was abnormal. Up-regulated actin-binding *Anxa2* and its calcium-binding partner *S100a10* are responsible for BTB integrity (Chojnacka et al. 2017). Interconnected *Atp1a1* (Fig. 4B), encoding Na/K-ATPase regulating gap junction (Rajamanickam et al. 2017), and *Gja1*, encoding one of the main gap junction proteins connexin 43 (Sridharan et al. 2007), were down-regulated. Up-regulated *Cdc42* (Fig. 4B) encodes a Rho GTPase governing cell polarity and maintaining BTB (Heinrich et al. 2021).

This molecular evidence of Sertoli cell spatial organization disturbance and disruption of cell contacts is in good agreement with the patterns observed during histological examination. We further confirmed this finding by immunofluorescent staining for vimentin (Fig. 4C) and observed the lack of vimentin polymerization concomitant with disruption of intercellular contacts and loss of BTB integrity. Moreover, it agrees with the results of the DAVID functional annotation tool performed by de Gendt et al. (De Gendt et al. 2014) for SCARIBO mice.

Therefore, our findings on differential gene expression in Sertoli cells are in agreement with data obtained in mice with impaired AR signaling. Among the top enriched biological processes several up-regulated stress response pathways were found, indicating deterioration of the Sertoli cells in the absence of testosterone (Fig. 4D).

Germ cells

As primary spermatocytes of double knockout mice stop developing in pachytene, we compared gene expression in two groups of germ cells: undifferentiated spermatogonia and meiosis-entry (leptotene-zygotene-pachytene) spermatocytes. 1 107 DEGs were identified for undifferentiated cells, 1 650 for spermatocytes, and 874 of these genes were common. Almost all the DEGs were up-regulated (99.2%). This overlap may be explained by the fact that undifferentiated and differentiated spermatogonia represent a continuous spectrum with gradually changing transcription patterns. Unique genes for the Early Spermatogonia cluster were attributed by GO as genes related to RNA processing and biosynthesis and ribosome biogenesis, whereas no stem cell specific pathways were found. We conclude that *Cdk8/19* knockout and disruption of steroid biosynthesis in testosterone production have no significant impact specifically on early spermatogonia. Pachytene is the most advanced stage observed in knockout testes and it is

followed by cell death. Accordingly, apoptosis-related pathways, stress response pathways and the autophagy pathway were upregulated (Supplementary Table S3, Supplementary Fig. S4). More specifically, a set of meiosis-specific genes were also up-regulated. These genes were related to chromosome pairing, DNA recombination and histone modification, which are known to be involved in meiosis. We hypothesize that this effect might be caused by compensatory mechanisms triggered by inability to proceed through meiosis.

Validation of single cell RNA data

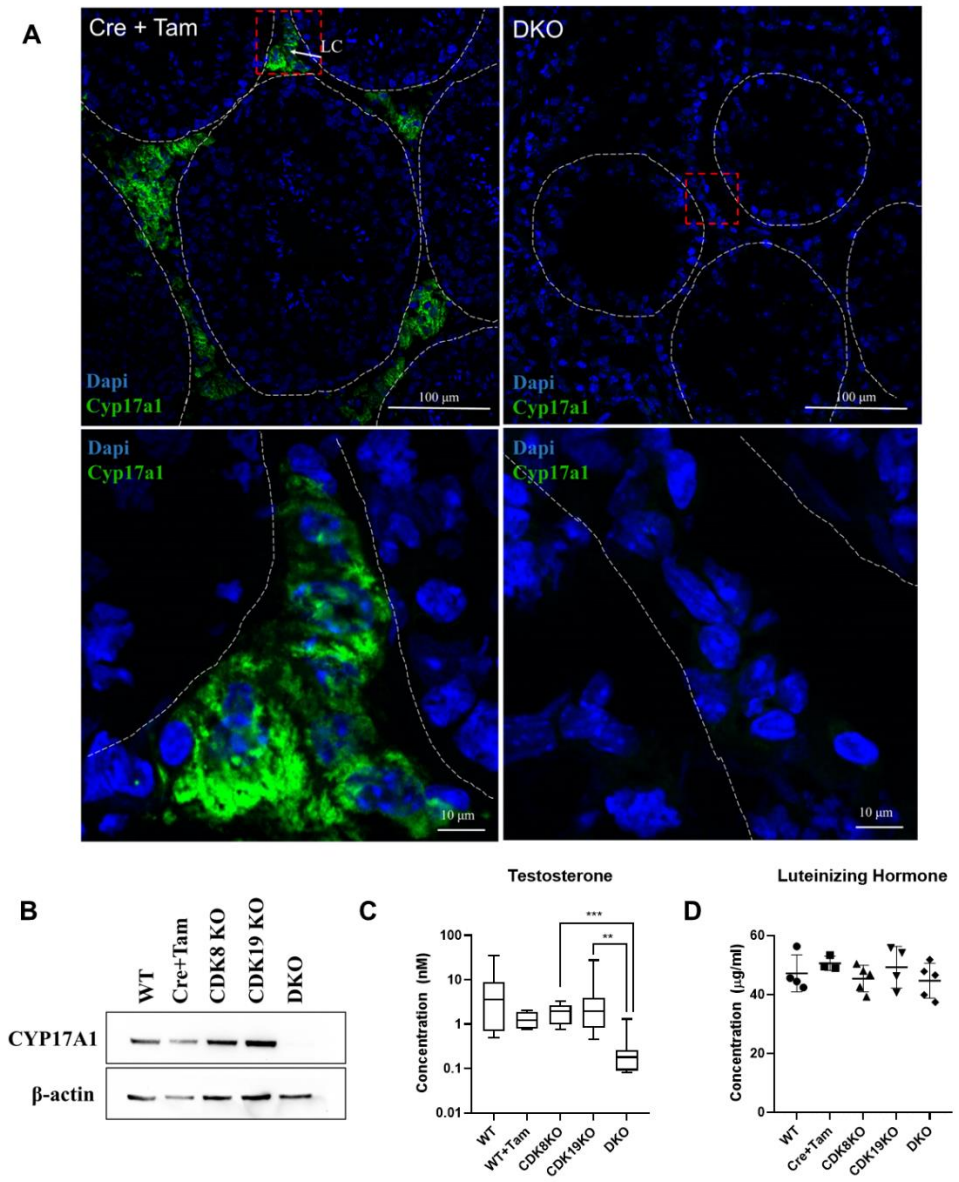

Figure 5. Confirmation of single cell RNA sequencing data with other methods. *(A)* IF staining for CYP17A1 of testis frozen sections, magnification 600X. CYP17A1 is visualized in extratubular space in Leydig cells in control mice and is completely absent in DKOs. *(B)* Western blot for CYP17A1 confirms disappearance of the protein in DKOs, but not in other genotypes. *(C)* In agreement with this testosterone blood level is decreased only in DKO mice. *(D)* Luteinizing hormone production is not impaired by CDK8 KO and CDK19 KO or DKO.

To further prove the steroid hypothesis we performed CYP17A1 immunostaining of testicular cross sections and western blotting, as well as direct testosterone measurement in the blood via LC-MS and cell culture experiments with ex vivo Leydig cells.

In the frozen sections of control mouse testis, CYP17A1 protein was localized outside of seminiferous tubules, in Leydig cells. In DKO animals, CYP17A1 staining was completely absent (Fig. 5A), despite Leydig cells being present in histological sections (Fig. 1G). WB (Fig. 5B) further confirmed this finding.

CYP17A1 catalyzes several key reactions leading to transformation of pregnenolone into testosterone. We measured the concentration of the key androgen hormone - testosterone in the blood of wild-type mice, single CDK8 KO and CDK19 KO and DKO. Only DKO showed significantly lower levels of testosterone, consistent with only this genotype presenting abnormal spermatogenesis (Fig. 5C).

Changes in steroid synthesis in Leydig cells can be caused by several mechanisms – specifically CDK8/19/Cyclin C can regulate CYP17A1 expression in Leydig cells themselves, or CDK8/19/Cyclin C may be involved in regulation of brain hormonal signals, which control testosterone production. To test the latter hypothesis we measured the concentration of luteinizing

hormone in blood serum. The results showed no difference in LH level through all the genotypes (Fig. 5D). This means that CDK8/19/Cyclin C acts directly in Leydig cells to regulate steroidogenesis.

Spermatogenesis in CDK8/19 DKO mice slightly recovers with time

To address the question of the persistence of spermatogenesis failure we performed histological and flow cytometry analysis of mice 5 months after tamoxifen-treatment. A certain percentage of 1n cells (primarily round spermatids) have reappeared 3-5 months after tamoxifen treatment (Fig. 6A), nevertheless the total number of cells and 1n cells remained low compared to control (Fig. 6B). H&E staining of prostate and epididymis also revealed slight alleviation of the phenotype, but no mature sperm (Fig. 6C). Immunofluorescent staining of seminiferous tubules confirmed this finding demonstrating solitary tubules with postmeiotic cells (Fig. 6D). However, CYP17A1 was not restored in Leydig cells (Fig. 6E).

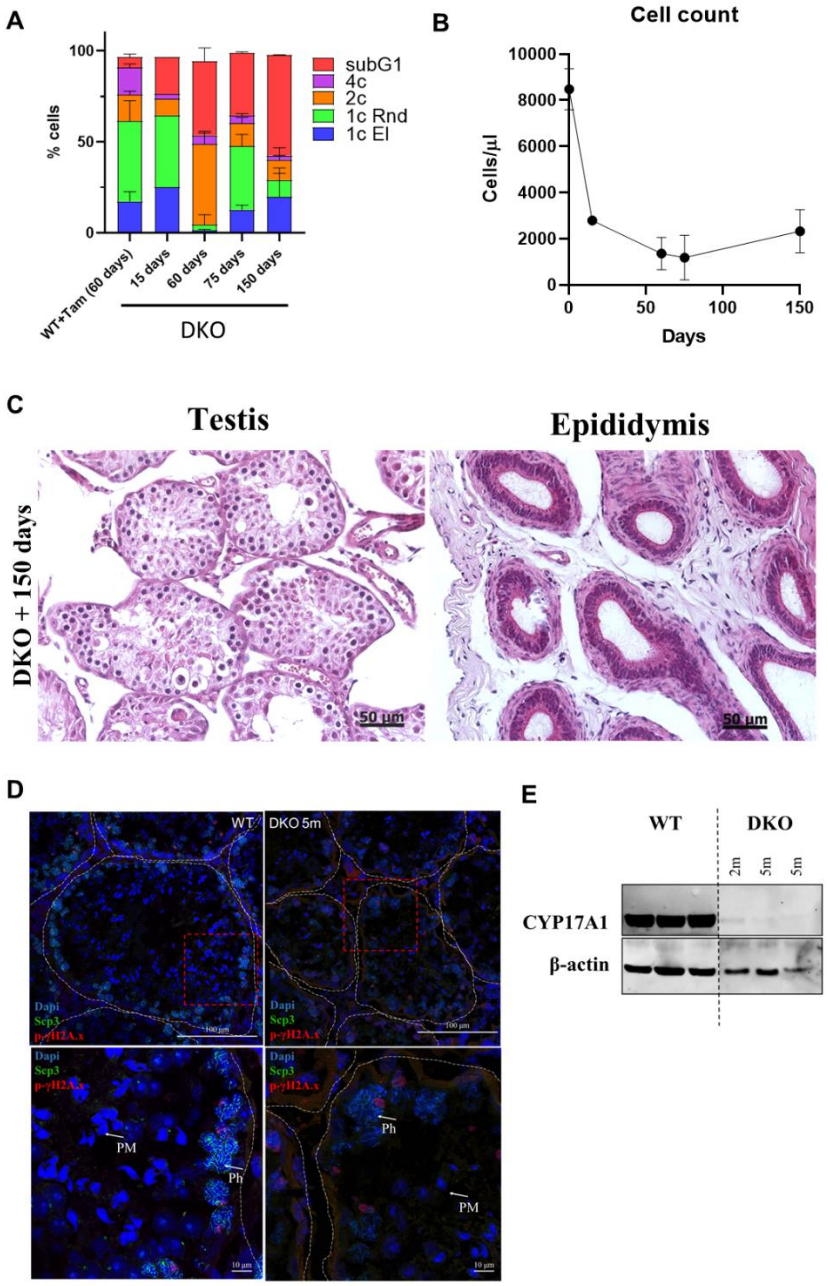

Figure 6. A minor recovery of spermatogenesis 5 months after DKO induction. *(A)* Round and elongated spermatids are once again detected by flow cytometry 5 months after DKO, however, *(B)* overall testis cellularity is only slightly increased. *(C)* Postmeiotic cells become visible at H&E staining of the tubules, however, epididymal ducts remain empty. *(D)* Post-pachytene and post-

meiotic (PM) cells became visible on the SYCP3 + γH2A.X stained frozen sections, magnification 600X. *(E)* CYP17A1 level remains at the background level 5 months after KO induction.

Pharmacological inhibition of CDK8/19 does not affect spermatogenesis

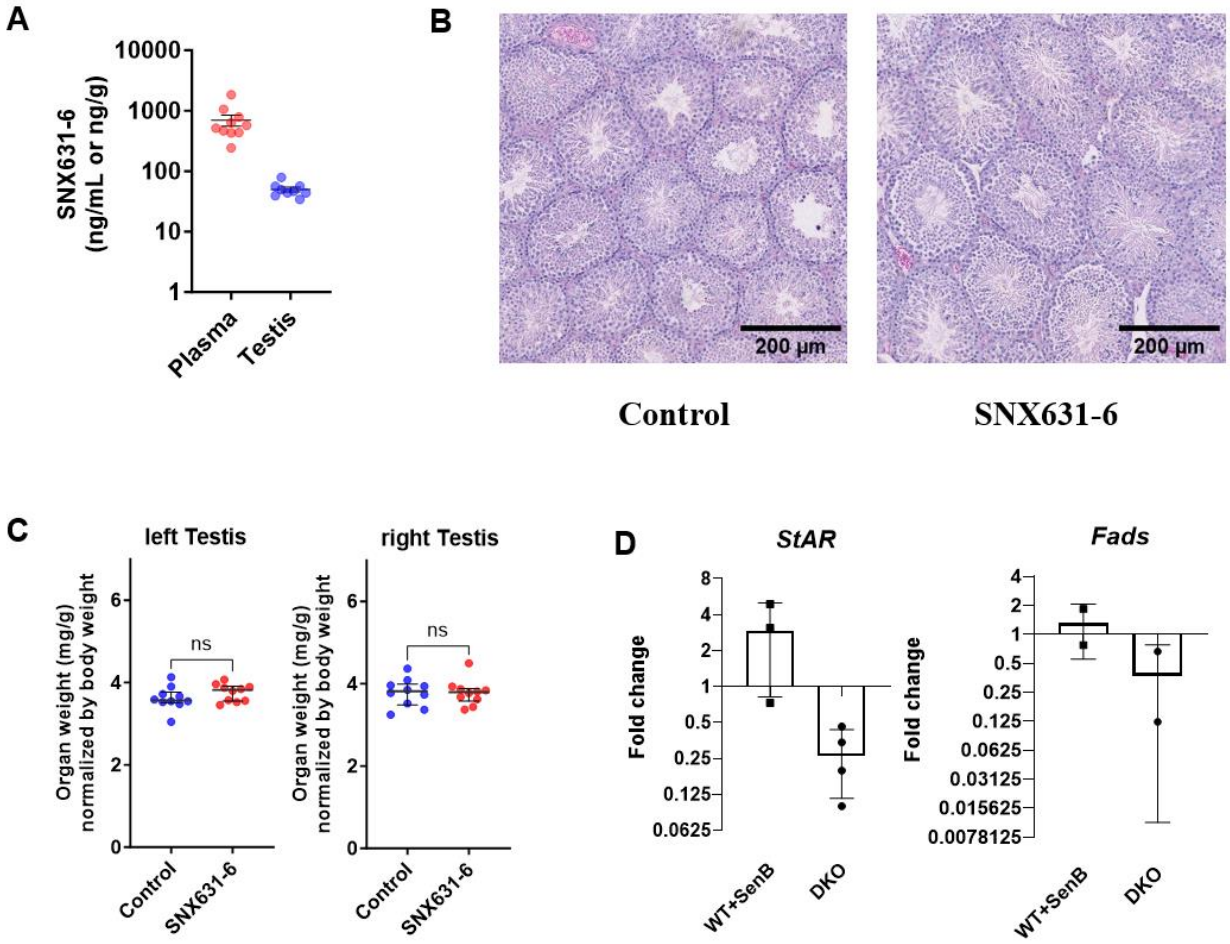

Figure 7. Effects of CDK8/19 inhibitor on spermatogenesis in mice *(A-C)* male C57BL/6 mice were treated with SNX631-6 medicated chow (500 ppm, 40-60 mg/kg/day dosage on average) for three weeks. *(A)* SNX631-6 concentrations in plasma and testis tissues at endpoint. *(B)* Representative images of H&E histology analysis of the testis tissues collected from animals in control or treated groups. *(C)* organ weights of testis (left and right) at endpoint. *(D)* qPCR analysis

of steroidogenic *Star* and *Fads* genes in ex vivo cultured Leydig cells in response to CDK8/19i Senexin B (1 μM) or hydroxytamoxifen-induced CDK8/19 DKO.

Recent findings have established that CDK8/19 may have kinase-independent functions (Steinparzer et al. 2019). One of such proposed mechanisms is stabilization of Ccnc by CDK8/19 (Chen et al. 2023). Depletion of CDK8/19 in testis leads to Ccnc degradation (Fig. 1C). To examine if the observed phenotype is related to the kinase activity of CDK8/19 or is kinase-independent we treated WT mice with a pharmacological CDK8/19 inhibitor – SNX631-6 (Li et al. 2023). 11 weeks old male C57BL/6 mice were treated with SNX631-6 medicated chow (500 ppm, 40-60 mg/kg/day dosage on average) or control diet for 3 weeks. No abnormal clinical observations were identified in treated mice through the whole treatment period. At the end of the experiment, the drug concentration in plasma and testis tissue were determined by LCMSMS (Fig. 7A). Testis tissues were weighed and fixed in 10% formalin for H&E staining. There were no significant difference in testis tissue weight between control and treated group and histology analysis did not reveal any noticeable difference (Fig. 7B,C), in contrast to the testis tissue of CDK8/19-DKO mice. While the drug concentration in the testis was lower than in blood, suggesting the effects of the blood-testis barrier, the average drug concentration in the testis was 50 ng/ml, which is ~10 times higher than the drug's IC_{50} in the cell-based assay.

The effects of DKO and CDK8/19 kinase inhibition were compared in *ex vivo* primary Leydig cell culture from WT mice and *Cdk8*$^{fl/fl}$*Cdk19*$^{-/-}$*Cre-Rosa* mice. We treated the first with CDK8/19 inhibitor Senexin B and the latter with hydroxytamoxifen to induce *Cdk8*$^{-/-}$ in vitro. Then we performed RT PCR to compare expression levels of several steroidogenic genes downregulated according to single cell RNA sequencing data: *Cyp17a1*, *Star* and *Fads* in treated and untreated

cells (Fig. 7D). *Star* and *Fads* were downregulated in OH-Tam treated cells, whereas basal *Cyp17a1* expression level was too low to make any conclusion. At the same time, CDK8/19 inhibition didn't affect expression levels of *Star* and *Fads*, suggesting that the effects of the DKO were kinase-independent.

Discussion

The Mediator complex is a key part of transcriptional regulation through signaling pathways, with numerous studies showing its role in different physiological processes. In recent years the enzymatic component of the Mediator-associated CKM module – CDK8 and its paralog CDK19, have emerged as co-regulators in several signal-activated transcriptional pathways, such as Wnt, TGF-beta, androgen and estrogen signaling, STATs, response to serum growth factors and others (reviewed in (Menzl et al. 2019)). Despite that, the knockout of *Cdk8* is only critical at the embryonic stage (Westerling et al. 2007), with no phenotype apparent in adult organisms (McCleland et al. 2015), while *Cdk19* is dispensable both at the embryonic and postnatal stages. The same tendency is observed for the knockout of MED subunits and other CKM proteins: constitutive KOs are most often embryonically lethal (except for an apparently less important paralog of MED12 - MED12L), and very few of them are described with a severe phenotype (Ilchuk et al. 2023).

It was proposed that CDK8 and CDK19 can replace each other, and therefore compensate for the effect of their counterpart in KO animals. To confirm this hypothesis we obtained the first ubiquitous knockout of *Cdk8/19* in 2 months old animals. If CDK8 and CDK19 functions are redundant, DKO would show a phenotype that is not produced by the knockout of *Cdk8* or *Cdk19* alone. Previously described animals with conditional knockout of *Cdk8* in the intestine on *Cdk19*$^{-/-}$ background presented with a mild phenotype, moderately affecting the number of specialized secreting cells (Dannappel et al. 2022). At the same time, our DKO mice had a phenotype evident at the histological level: they lacked haploid spermatids and mature spermatozoa (Fig. 1F). Further histological examination revealed that primary spermatocytes were blocked in pachytene of meiosis I (Fig. 2). Surprisingly, careful examination of *Cdk8*$^{-/-}$ males previously described as

asymptomatic revealed their complete infertility due to the lack of sexual behavior, despite the absence of morphological changes in the urogenital system (Fig. 1E). Tamoxifen used for KO induction is an estrogen receptor modulator and can affect the mouse organism, especially fertility and hormonal levels, per se (Willems et al. 2011). Previously, we found it unsuitable for studying KOs in the female reproductive system (Ilchuk et al. 2022). To ensure that observed effects are caused by the KOs and not by tamoxifen treatment we used tamoxifen-treated controls in every experiment and conducted all experiments but one (Fig. 1D) at least one month after tamoxifen treatment. We demonstrated that in our experiments tamoxifen does not reduce male fertility nor does it impact hormonal levels.

An opposed to the phenotype described here, a defect of spermatogenesis, however not affecting fertility, was previously noticed in Med1$^{fl/fl}$/Vasa-Cre tissue specific KO: prophase I passage was accelerated in these mice and spermatocytes entered zygotene/pachytene stage prematurely (Huszar et al. 2015). The difference between these effects is quite interesting in the context of the concept that association with CKM attenuates Mediator-dependent transcription either by sterically preventing TF binding (Freitas, K.A.; Science 2022), or by post-transcriptional regulation of Mediator complex subunits (Poss et al. 2016; Chen et al. 2023). As far as we know, besides the current work, Huszar et al (2015) is the only paper establishing a connection between any components of the Mediator complex and spermatogenesis.

Here we demonstrated a disruption of steroid biosynthesis in Leydig cells which could play the key role for the observed phenotype. As opposed to spermatogenesis, a number of works (reviewed in (Ilchuk et al. 2023)) affirm a significant role of Mediator complex in lipid metabolism and biosynthesis as one of the main cofactors for main adipogenic TFs such as C/EBPα, PPARγ and SREBP.

Initially we detected a decrease in steroidogenic activity by single cell RNA sequencing and then confirmed it by WB, immunofluorescence, and direct testosterone measurement. *Cyp17a1* gene, encoding the key steroidogenic enzyme converting progestogens to androgens, was downregulated 10-fold in Leydig cells (Fig. 3D). At the same time, the corresponding protein, CYP17A1, dropped almost to the undetectable level (Fig. 5B). LC-MS measurement also confirmed decrease of serum testosterone level in DKO mice. This corresponds well with perturbed Leydig cells morphology (reduced size and secretory vacuoles depletion) and explains observed atrophy of prostate and epididymis (Fig. 1F). It is worth mentioning that constitutive *Cyp17a1* knockout in mice leads to female phenotype in XY mice (Aherrahrou et al. 2020). Besides *Cyp17a1*, several other steroid metabolism related genes were downregulated (*Lcn*, *Fads*, *Star*, *Sc5d*, *Sult1e1*). Interestingly, the main feature of *Fads* (Stoffel et al. 2008) and *Sult1e1* (Song 2007) KOs is male infertility, caused by spermatogenesis arrest at different stages.

There is much evidence that meiosis in spermatocytes depends on AR signaling (Wang et al. 2022). Several papers established a connection between AR signaling, and the Mediator complex (Russo et al. 2019). MED1 and MED19 directly interact with the AR and regulate its transcriptional activity (Jin et al. 2012; Weber et al. 2021). Additional evidence of the role of the Mediator complex and Cdk8/19 in the urogenital system comes from studies of their role in prostate cancer, where Cdk19 is elevated together with the AR (Becker et al. 2020).

Sertoli cells are the main driver of spermatogenic differentiation that receive testosterone signals from Leydig cells and convert them into more specific signals which are further transmitted to germ cells at different stages of the spermatogenic cycle. The CDK8/19 DKO has also dramatically impacted Sertoli cells.

The SCARKO mice were engineered two decades ago and show morphological abnormalities (i.e, reduced testis, epididymis and prostate, meiotic arrest during meiosis I prophase) similar to CDK/19 DKO (De Gendt et al. 2004; Chang et al. 2004). scRNAseq technique used to elucidate the molecular mechanism of the meiotic arrest revealed a number of similarities with DKO single-cell RNA seq data for Sertoli cells, especially in terms of pathways (Cao et al. 2021). Thus, genes associated with cytoskeleton, cellular membrane and cell-cell contacts were enriched among the DEGs (Fig. 4B). Nevertheless, the overlap of genes affected in the SCARKO and DKO mice was low (Supplementary Fig. S3). However, an important difference between our model and SCARKO is that *Cdk8* knockout is induced after puberty. Another important consideration is that Sertoli cells are not the only cell type impacting spermatogenesis through AR signaling. AR signaling in peritubular myoid cells is also essential for successful spermatogenesis (Welsh et al. 2009) . In this regard, probably a more relevant model for comparison with our results is described in (Stanton et al. 2012) where androgens were manipulated chemically in grown-up rats. In this paper the most impacted group displayed apoptosis of a fraction of spermatocytes and full blockage of second meiotic division.

Just as in Stanton et al. (2012), genes differentially expressed in spermatocytes blocked in prophase I can be divided in the following groups: (1) genes with known roles in meiosis, especially DNA synapse, homologous recombination and DNA repair, (2) genes associated with cellular stress and apoptosis, and (3) genes with roles in RNA processing and splicing. Changes in the first group can be explained by the compensatory mechanisms and changes in the second group correlate well with the observed extensive cell death of spermatocytes, changes in the third group remain enigmatic.

Noteworthy, 99.2% of spermatocyte DEGs with |logFc|>0.4 were upregulated genes, which is very similar to the findings of Pelish et al. (Pelish et al. 2015) and agrees with the negative regulation of the Mediator complex by CDK8/19 (Chen et al. 2023).

Based on these results we can conclude that DKO causes perturbance in different testicular cell types: Leydig cells, Sertoli cells and spermatocytes. We hypothesize that all these changes are caused by disruption of testosterone synthesis in Leydig cells. Data for another cell type are consistent with this hypothesis, however there is still a possibility that CDK8/19 have distinct roles in other testicular cell types which are not visible against the background of the prominent lesions of the Leydig cells. However, our data are not sufficient to make the conclusion about the role of CDK8/19/Cyclin C directly in meiosis, besides its hormonal regulation. To answer this question, definitive mouse strains with cell-type specific KO in Sertoli cells and meiotic spermatocytes would be needed.

The effects of CDK8/19 DKO on spermatogenesis were maximal at 1-2 months after tamoxifen administration. At later time points we detected partial restoration of spermatogenesis, and signs of re-differentiation of the epididymis and activity of secreting cells in the prostate. This restoration did not lead to the production of mature sperm, and the total number of haploid cells increased insignificantly. There are several possible explanations for such an effect. It is unlikely that restoration happened in cells, which did not activate Cre-Lox, as the absence of CDK8 has been confirmed by us through PCR (Supplementary Figure S1A). Additionally, no restoration of CYP17A1 was found in 5-month-old animals. There is a possibility that transcription of genes previously regulated by CDK8/19/Cyclin C was rewired through other transcriptional regulators. An intriguing possibility is activation of a compensatory AR-independent pathway that was recently shown in a zebrafish model (Zhai et al. 2022). Such signaling involves increased progestin

signaling, and upregulation of 17α,20β-Dihydroxy-4-pregnen-3-one. An argument against such hypothesis would be the absence of such compensation in *Cyp17a1* KO animals or SCARKO mice, but in the former animals the male reproductive system does not develop at all, and in the latter, non-canonical AR signaling through Src kinase may lead to progression to round spermatid stage (Cooke and Walker 2021).

The luteinizing hormone produced in the pituitary gland is a major regulator of steroidogenesis in Leydig cells. It was shown that LH regulates expression level of *Cyp17a1* and several other steroidogenic genes (Li et al. 2021; Ma et al. 2004). As CDK8 KO in our model is ubiquitous, infertility could be caused by decrease of LH level due to improper regulation in the brain. However, we measured LH level in the serum and found it unaffected by single or double KOs (Fig 5D). That means that CDK8/19/Cyclin C are required for steroidogenic genes transcription in Leydig cells. And indeed, in our ex vivo experiment with Leydig primary cell culture, even without addition of LH, expression of *Star* and *Fads* was downregulated upon in vitro induction of *Cdk8* KO by hydroxytamoxifen on the *Cdk19*$^{-/-}$ background. We anticipated to detect the same decrease of *Cyp17a1* expression, however in the absence of hormonal stimulation only very low *Cyp17a1* levels at the margin of error were detectable.

The results of the present study reveal for the first time the role of CDK8/19/Cyclin C in spermatogenesis and, more generally, in the function of the male reproductive system. The key question regarding the results described here, or any other results observed upon the knockout or knockdown of *Cdk8/19*, is whether the phenotypic effects are due to the inhibition of CDK8/19 kinase activity or to the loss of Cyclin C, which is protected by CDK8 and CDK19 from proteasome-mediated degradation, in a kinase-independent manner (Chen et al. 2023). Here we show that Cyclin C essentially disappears both from the embryo fibroblasts and from the testes of

the DKO mice. Given the known CDK8/19-independent functions of Cyclin C (Ježek et al. 2019), and the effect of Cyclin C knockout on lipid accumulation (Song et al. 2022), the likelihood of Cyclin C rather than CDK8/19 mediating the observed effects should be investigated. As we have shown, 30-day treatment of 11 weeks old mice with a potent CDK8/19 kinase inhibitor produced no anatomical changes in the testes. Furthermore, ex vivo treatment of Leydig cells with a CDK8/19 inhibitor did not reproduce of DKO on gene expression, suggesting that the effects of DKO were kinase-independent and possibly mediated by Cyclin C. A definitive answer to the role of Cyclin C *vs* CDK8/19 kinase activity will require a phenotypic comparison of DKO mice with mice expressing kinase-inactive mutants of CDK8/19 or inducible Cyclin C knockout.

Materials and Methods

Animals and conditional Cdk8/19 DKO

Cdk8$^{fl/fl}$ and R26-Cre-ER^{T2} (Jax 008463; B6.129-Gt(ROSA)26Sor$^{tm1(cre/ERT2)Tyj/J}$) provenance and genotyping were performed as described (Ilchuk et al. 2022). *Cdk19*$^{-/-}$ (*Cdk19*$^{em1(IMPC)J}$) were purchased from Jackson Laboratory. Animals were maintained under controlled room conditions (22–24°C and a 14 h light: 10 h dark photoperiod). Mice were given access to food and water *ad libitum*. All manipulations with animals were performed according to the Local Bioethical Committee recommendations and according to the Declaration of Helsinki (1996).

Mice were genotyped by real-time PCR using oligonucleotides listed in Supplemental Table S3. Tamoxifen treatment was performed as described previously: 8-10 week old males were injected with 3 mg of tamoxifen daily for 7 consecutive days (Ilchuk et al. 2022). Mice were sacrificed by cervical dislocation. To evaluate fertility, males were kept with two CD-1 outbred female mice each. Copulative plugs and newborn pups were monitored daily in the morning.

Histology

For primary tissue examination organs were fixed in 10% formaldehyde, paraffin embedded, sectioned on a microtome and stained with H&E.

For immunofluorescent staining frozen sections were used. Organs were collected in tissue freezing medium (Leica Biosystems, Germany). Sections were cut 3 μm thick in the cryostat at −20°C. Slides were incubated for 2 min in 4% PFA and washed with PBS three times for 10 min. Sections were permeabilized in 0.03% Triton-X100 (VWR Life Science, Radnor, PA), 0.1% rabbit serum diluted in PBS at 4°C overnight and washed again with PBS. Sections were stained with

primary antibodies (Supplemental Table S3) at a dilution of 1:100 for an hour, washed in PBS, and incubated with secondary antibodies (1:100). Slides were stained with 5 ng/ml DAPI (Thermo Fisher Sci., Waltham, MA), mounted with Mowiol® 4-88 (Sigma-Aldrich) and examined on Leica STELLARIS confocal microscope (Leica Microsystems, Germany).

Flow cytometry spermatogenesis assay

The protocol modified from (Jeyaraj et al. 2003) was used. The testes of mature mice were placed in phosphate buffered saline (PBS), the albuginea was opened, and the contents were transferred to a solution of 0.5 µg/ml collagenase IV (PanEco, Russia) in PBS and incubated for 15 min at 32°C with shaking at 220 rpm. The seminiferous tubules were washed twice with 1 U DNAse (NE Biolabs, Ipswich, MA) in PBS, transferred to 0.01% trypsin (PanEco), and shaked for 15 min at 32°C, 220 rpm. Trypsin was inactivated with 0.01% bovine serum albumin in PBS; cells were thoroughly resuspended, passed through 70 µm nylon cages (Wuxi NEST Biotechnology, China) and reconstituted in 1 ml PBS. For flow cytometry cells were fixed with 0.75% PFA for 15 minutes at 37°C, then washed in PBS. Cells were lysed in the buffer containing 50 µg/ml propidium iodide (PI), 100 µg/ml RNAse A, 0.1% sodium citrate, 0.3% NP-40 (VWR Life Science) for 30 min at 4°C in the dark followed by flow cytometry analysis on a CytoFlex 26 (Beckman Coulter, Indianapolis, IN) in PE-A and PerCP-A channels. At least 10,000 fluorescent ‘events’ were collected per each sample. Data were analyzed using CytExpert software (Beckman Coulter).

10x Chromium library preparation and sequencing

2 R26-Cre-ER^{T2} and 2 *Cdk8*$^{fl/fl}$*Cdk19*$^{-/-}$R26-Cre-ER^{T2} tamoxifen-treated male mice at 7th week after activation were sacrificed and tissue cell suspension was prepared as described above. Single cell 3' v3 kit and Chromium controller (10X Genomics) (Zheng et al. 2017) were used to generate GEMs for further processing. RT and other stages of single cell library preparation were performed as per manufacturer instructions, with the exception of AMPure XP Reagent used instead of SPRIselect. These sample libraries were sequenced with Illumina Novaseq6000.

Single cell data processing

Raw fastq files generation, alignment and read filtering were done by 10x Genomics Cell Ranger 6.1.1 with default settings. Read quality was additionally assessed with FastQC. Reads were aligned to the GRCm38 genome, with an average 95% alignment rate. Raw counts, generated by Cell Ranger 6.1.1, were piped to Seurat (Hao et al. 2021), where additional filtering was applied. Cells with aberrant UMI vs. genes relations were filtered with pagoda2 genes vs. molecule filter (https://github.com/kharchenkolab/pagoda2), where minimal counts were set as 1000 and minimal genes as 500. Next, cells with high percentages of mitochondrial genes expressions per cell were excluded, threshold for filtering set as 25%. After that Scrublet doublet (Wolock et al. 2019) score was calculated, cells with scores higher than 0.20 were marked as doublets and excluded. Each sample had more than 5000 high quality cells remaining after filtering. These cells were normalized with the default Seurat method and piped to further filtering and analysis.

To account for ambient gene expression, DecontX (Yang et al. 2020) was used, for which cluster-assigned data is required. For stable cluster assignment, a reference dataset was formed of WT samples, which were integrated via Harmony (Korsunsky et al. 2018) and then clustered with

Seurat. Clustering was checked against testis cell type markers (Hermann et al. 2018; Cao et al. 2021) to ensure selection of true clusters that would reiterate across samples. Cluster of cells belonging to the IGB_2 WT sample only, which did not correspond to any cell type and was missing essential housekeeping genes, was discarded as a cluster of low quality cells with no biological relevance. This reference dataset was used for automatic cluster mapping with Seurat for all samples, and received labels were used with DecontX to lessen share of ambient gene expression in data.

Single cell data analysis

Corrected counts for all cells were piped back to Seurat. Then normalized WT and double knockout samples were integrated with Harmony to account for samples' batch effects. 3480 variable genes were used for PCA and following integration, none of them mitochondrial or ribosomal. Harmony-integrated data was UMAP dimension-reduced and clustered with Seurat. Visualizations were also made with the Seurat package. Cell type was assigned according to their marker genes (Hermann et al. 2018; Cao et al. 2021). Both cells and microenvironment in the testis were detected in wild-type as well as in KO samples.

Spermatogonia cell cluster was reintegrated and reclustered separately for discovery of spermatogonia subtypes. Integration and clusterization was done as before, with 798 features at the start of the process. Spermatogonia subclusters were assigned types according to literature-curated marker genes (Hermann et al. 2018; Cao et al. 2021). Differential expression tests (negative binomial Seurat implementation) were conducted for each chosen cell cluster with WT compared against double knockout, batch effect between samples accounted for with the linear model. All mitochondria, ribosomal and high ambient genes (by DecontX) were excluded from

testing. Genes with absolute logFC < 0.4 and genes expressed in less than 20% cells in class were excluded either. Additionally, after testing, all genes with no or almost no expression in double knockout, high expressions in WT, and high expression in WT spermatids were excluded as their differential expression might be caused by different ambient composition in WT, heavily influenced by larger spermatid cell proportion. For Sertoli cells, a small subcluster, potentially caused by technical effects, was excluded before testing.

Assignment of groups and cell count

The clustering analysis was performed according to markers described in previous studies (reviewed in (Suzuki 2023)). This analysis allowed us to identify nine populations with respective genes: Sertoli cells (*Wt1, Sox9, NR5a1, Clu*), Leydig cells (*Hsd3b1, Cyp17a1*), macrophages (*Cd74, C1qa, Cd45, Ccl5*), T-cells, fibroblasts (*Pdfrgfra, Cd34, Dcn, Gcn*), and the differentiating sperm lineage divided into 5 clusters: undifferentiated/early spermatogonia (*Crabp1, Tcea3, Kit*), meiotic entry (*Stra8, Rhox13*) leptotene/zygotene (*Sycp3, Dmc1*), two clusters for pachytene (*Piwil1, Id4*) and pachytene/diplotene (*Acr, Pgk2*) (Supplementary Fig S5).

Hormone measurement

To measure the concentration of hormones in the serum, blood was taken from the left ventricle of the heart, transferred to sterile test tubes and left at 4°C overnight. Measurement of luteinizing hormone was performed using ELISA (CEA441Mu, CloudClone, China). The testosterone concentration was measured by the LC-MS method as described previously (Povaliaeva et al. 2020). 17α-Hydroxyprogesterone-d8 were used as standard, proteins were precipitated by adding $ZnSO_4$ and MeOH. The measurement was performed using an on-line

extraction method with Agilent Bond Elut C18 cartridges as trap column and Waters Aquity UPLC BEH C18 column, Agilent 1290 Infinity II LC and and AB Sciex Triple Quad 5500 mass-spectrometer.

Immunoblotting

Protein lysis and western blotting were performed as described in (Ilchuk et al. 2022). Briefly, cells were lysed in RIPA buffer supplemented with protein inhibitor cocktail (Sigma-Aldrich, St. Louis, MO). Total protein concentration was quantified by the Bradford method. Absorbance at 560 nm was measured with a CLARIOstar Plate Reader (BMG Labtech, Germany). Proteins were separated by SDS-PAGE and transferred onto 0.2 μm nitrocellulose membrane (Bio-Rad, Hercules, CA). After blocking with 5% skimmed milk, membranes were treated with primary antibodies (Supplementary table S3) and incubated at 4°C overnight. Membranes were washed with Tris-borate saline with Tween 20 (TBS-T) and incubated for 1 h at room temperature with secondary antibodies (Supplementary table S3). Membranes were visualized with the Clarity Western ECL Substrate (Bio-Rad) using a iBright FL1500 Imaging System (Invitrogen, Waltham, MA).

Leydig cell culture

Seminiferous tubules were isolated as described above for flow cytometry but after collagenase IV (1 ug/ml) digestion the supernatant was passed through 70 μm nylon cages and centrifuged at 1000 rpm. The cells were resuspended in the medium for Leydig cells (low glucose DMEM (PanEco) with 10% fetal bovine serum (FBS, HyClone, GE Healthcare Life Sciences, Chicago, IL), 1% penicillin/streptomycin (PanEco), 0.3 mg/ml *L*-glutamine (PanEco)) and seeded

on Costar® 6-well plates (Corning, New York, NY) pre-coated by 0.01% poly-*L*-lysyne (Sigma-Aldrich, P0899), incubated at 37ºC in 5% CO_2 for 1 h and carefully washed with the medium. After 24 h cells were treated with 0.56% potassium chloride hypotonic solution for 5 min to remove unattached cells. On the 7th day 1 μM Senexin B (SenB, Senex Biotechnology, Columbia, SC) or 1 μM 4-hydroxytamoxifen (4-OHT, Sigma-Aldrich) was added to the cells. After 7 days of incubation, the cells were lysed with ExtractRNA (Evrogen, Russia).

qRT PCR

Total RNA from cell suspension was extracted with ExtractRNA and quantified using NanoDrop. Equal amounts of RNA were reverse-transcribed to generate cDNA using Superscript II reverse transcription Supermix for qRT-PCR (Invitrogen). qRT-PCR was then performed with SYBR PCR Mix (Evrogen) using the Thermal Cycler system (Bio-Rad). The data thus obtained were analyzed following the comparative (ΔΔCt) method. *Actb* was used as a housekeeping gene. Sequences of primers used are listed in Supplementary Table S3.

Statistics

One-way or two-way analysis of variance (ANOVA) followed by Sidak's post hoc test for multiple comparisons was used (GraphPad Prism 9; GraphPad Software, San Diego, CA). P value <0.05 was taken as evidence of statistical significance.

Competing Interest Statement

I.B.R is Founder and President and M.C. is consultant of Senex Biotechnology, Inc. Other authors declare no conflict of interest.

Acknowledgments

Animal experiments, single cell RNA sequencing and histology were funded by Russian Science Foundation project #22-15-00227. Flow cytometry and confocal microscopy experiments were performed at the equipment of Center for Precision Genome Editing and Genetic Technologies for Biomedicine and funded by the Ministry of Science and Higher Education of the Russian Federation (075-15-2019-1661). We thank Dr. Andrey Yu. Kulibin for providing anti-SYCP3 antibodies and Tamara A. Kiriukhina for assistance in isolating of primary MEF culture.

Author contributions: A.B., E.V., N.S.., V.N.M., A.T., D.K., A.K., M.U., A.N., J.L., M.C., V.A.M. and V.T. carried out the experiments. A.B. wrote the manuscript with support from V.T. and E.V. E.V. designed the figures. E.V., A.K., I.R., M.C. and A.S. edited the manuscript. A.B., V.T., E.V., V.N.M. and Y.S. analysed the data. Z.A., V.B., D.O. and E.A. designed the computational framework and analysed the scRNA data. I.R. and A.S. conceived the original idea. A.B., I.R., A.S. and Y.S acquired the funding. A.B. and V.T. designed experiments, interpreted data and were the project administrators.

References

Aherrahrou R, Kulle AE, Alenina N, Werner R, Vens-Cappell S, Bader M, Schunkert H, Erdmann J, Aherrahrou Z. 2020. CYP17A1 deficient XY mice display susceptibility to atherosclerosis, altered lipidomic profile and atypical sex development. *Sci Rep* **10**: 8792. doi:10.1038/s41598-020-65601-0.

Alarcón C, Zaromytidou A-I, Xi Q, Gao S, Yu J, Fujisawa S, Barlas A, Miller AN, Manova-Todorova K, Macias MJ, et al. 2009. Nuclear CDKs drive Smad transcriptional activation

and turnover in BMP and TGF-beta pathways. *Cell* **139**: 757–769. doi:10.1016/j.cell.2009.09.035.

Aranda-Orgilles B, Saldaña-Meyer R, Wang E, Trompouki E, Fassl A, Lau S, Mullenders J, Rocha PP, Raviram R, Guillamot M, et al. 2016. MED12 Regulates HSC-Specific Enhancers Independently of Mediator Kinase Activity to Control Hematopoiesis. *Cell Stem Cell* **19**: 784–799. doi:10.1016/j.stem.2016.08.004.

Audetat KA, Galbraith MD, Odell AT, Lee T, Pandey A, Espinosa JM, Dowell RD, Taatjes DJ. 2017. A Kinase-Independent Role for Cyclin-Dependent Kinase 19 in p53 Response. *Mol Cell Biol* **37**. doi:10.1128/MCB.00626-16.

Barette C, Jariel-Encontre I, Piechaczyk M, Piette J. 2001. Human cyclin C protein is stabilized by its associated kinase cdk8, independently of its catalytic activity. *Oncogene* **20**: 551–562. doi:10.1038/sj.onc.1204129.

Becker F, Joerg V, Hupe MC, Roth D, Krupar R, Lubczyk V, Kuefer R, Sailer V, Duensing S, Kirfel J, et al. 2020. Increased mediator complex subunit CDK19 expression associates with aggressive prostate cancer. *Int J Cancer* **146**: 577–588. doi:10.1002/ijc.32551.

Behr R, Sackett SD, Bochkis IM, Le PP, Kaestner KH. 2007. Impaired male fertility and atrophy of seminiferous tubules caused by haploinsufficiency for Foxa3. *Dev Biol* **306**: 636–645. doi:10.1016/j.ydbio.2007.03.525.

Cao C, Ma Q, Mo S, Shu G, Liu Q, Ye J, Gui Y. 2021. Single-Cell RNA Sequencing Defines the Regulation of Spermatogenesis by Sertoli-Cell Androgen Signaling. *Front Cell Dev Biol* **9**: 763267. doi:10.3389/fcell.2021.763267.

Chang C, Chen Y-T, Yeh S-D, Xu Q, Wang R-S, Guillou F, Lardy H, Yeh S. 2004. Infertility with defective spermatogenesis and hypotestosteronemia in male mice lacking the

androgen receptor in Sertoli cells. *Proc Natl Acad Sci U S A* **101**: 6876–6881. doi:10.1073/pnas.0307306101.

Chen M, Liang J, Ji H, Yang Z, Altilia S, Hu B, Schronce A, McDermott MSJ, Schools GP, Lim C-U, et al. 2017. CDK8/19 Mediator kinases potentiate induction of transcription by NFκB. *Proc Natl Acad Sci U S A* **114**: 10208–10213. doi:10.1073/pnas.1710467114.

Chen M, Li J, Liang J, Thompson ZS, Kathrein K, Broude EV, Roninson IB. 2019. Systemic Toxicity Reported for CDK8/19 Inhibitors CCT251921 and MSC2530818 Is Not Due to Target Inhibition. *Cells* **8**. doi:10.3390/cells8111413.

Chen M, Li J, Zhang L, Wang L, Cheng C, Ji H, Altilia S, Ding X, Cai G, Altomare D, et al. 2023. CDK8 and CDK19: positive regulators of signal-induced transcription and negative regulators of Mediator complex proteins. *Nucleic Acids Res* **51**: 7288–7313. doi:10.1093/nar/gkad538.

Chojnacka K, Bilinska B, Mruk DD. 2017. Annexin A2 is critical for blood-testis barrier integrity and spermatid disengagement in the mammalian testis. *Biochim Biophys Acta Mol Cell Res* **1864**: 527–545. doi:10.1016/j.bbamcr.2016.12.012.

Clarke PA, Ortiz-Ruiz M-J, TePoele R, Adeniji-Popoola O, Box G, Court W, Czasch S, El Bawab S, Esdar C, Ewan K, et al. 2016. Assessing the mechanism and therapeutic potential of modulators of the human Mediator complex-associated protein kinases. *Elife* **5**. doi:10.7554/eLife.20722.

Cooke PS, Walker WH. 2021. Male fertility in mice requires classical and nonclassical androgen signaling. *Cell Rep* **36**: 109557. doi:10.1016/j.celrep.2021.109557.

Dannappel MV, Sooraj D, Loh JJ, Firestein R. 2018. Molecular and in vivo Functions of the CDK8 and CDK19 Kinase Modules. *Front Cell Dev Biol* **6**: 171. doi:10.3389/fcell.2018.00171.

Dannappel MV, Zhu D, Sun X, Chua HK, Poppelaars M, Suehiro M, Khadka S, Lim Kam Sian TC, Sooraj D, Loi M, et al. 2022. CDK8 and CDK19 regulate intestinal differentiation and homeostasis via the chromatin remodeling complex SWI/SNF. *J Clin Invest* **132**. doi:10.1172/JCI158593.

De Gendt K, Swinnen JV, Saunders PTK, Schoonjans L, Dewerchin M, Devos A, Tan K, Atanassova N, Claessens F, Lécureuil C, et al. 2004. A Sertoli cell-selective knockout of the androgen receptor causes spermatogenic arrest in meiosis. *Proc Natl Acad Sci U S A* **101**: 1327–1332. doi:10.1073/pnas.0308114100.

De Gendt K, Verhoeven G, Amieux PS, Wilkinson MF. 2014. Genome-wide identification of AR-regulated genes translated in Sertoli cells in vivo using the RiboTag approach. *Mol Endocrinol* **28**: 575–591. doi:10.1210/me.2013-1391.

de Mattos K, Viger RS, Tremblay JJ. 2022. Transcription Factors in the Regulation of Leydig Cell Gene Expression and Function. *Front Endocrinol* **13**: 881309. doi:10.3389/fendo.2022.881309.

Dong W-W, Huang H-L, Yang W, Liu J, Yu Y, Zhou S-L, Wang W, Lv X-C, Li Z-Y, Zhang M-Y, et al. 2014. Testis-specific Fank1 gene in knockdown mice produces oligospermia via apoptosis. *Asian J Androl* **16**: 124–130. doi:10.4103/1008-682X.122592.

Esteban-Lopez M, Agoulnik AI. 2020. Diverse functions of insulin-like 3 peptide. *J Endocrinol* **247**: R1–R12. doi:10.1530/JOE-20-0168.

Galbraith MD, Andrysik Z, Pandey A, Hoh M, Bonner EA, Hill AA, Sullivan KD, Espinosa JM. 2017. CDK8 Kinase Activity Promotes Glycolysis. *Cell Rep* **21**: 1495–1506. doi:10.1016/j.celrep.2017.10.058.

Griffin DK, Ellis PJ, Dunmore B, Bauer J, Abel MH, Affara NA. 2010. Transcriptional profiling of luteinizing hormone receptor-deficient mice before and after testosterone treatment provides insight into the hormonal control of postnatal testicular development and Leydig cell differentiation. *Biol Reprod* **82**: 1139–1150. doi:10.1095/biolreprod.109.082099.

Hao Y, Hao S, Andersen-Nissen E, Mauck WM 3rd, Zheng S, Butler A, Lee MJ, Wilk AJ, Darby C, Zager M, et al. 2021. Integrated analysis of multimodal single-cell data. *Cell* **184**: 3573–3587.e29. doi:10.1016/j.cell.2021.04.048.

Heinrich A, Bhandary B, Potter SJ, Ratner N, DeFalco T. 2021. Cdc42 activity in Sertoli cells is essential for maintenance of spermatogenesis. *Cell Rep* **37**: 109885. doi:10.1016/j.celrep.2021.109885.

Hermann BP, Cheng K, Singh A, Roa-De La Cruz L, Mutoji KN, Chen I-C, Gildersleeve H, Lehle JD, Mayo M, Westernströer B, et al. 2018. The Mammalian Spermatogenesis Single-Cell Transcriptome, from Spermatogonial Stem Cells to Spermatids. *Cell Rep* **25**: 1650–1667.e8. doi:10.1016/j.celrep.2018.10.026.

Huszar JM, Jia Y, Reddy JK, Payne CJ. 2015. Med1 regulates meiotic progression during spermatogenesis in mice. *Reproduction* **149**: 597–604. doi:10.1530/REP-14-0483.

Ilchuk LA, Kubekina MV, Okulova YD, Silaeva YY, Tatarskiy VV, Filatov MA, Bruter AV. 2023. Genetically Engineered Mice Unveil In Vivo Roles of the Mediator Complex. *Int J Mol Sci* **24**: 9330. https://www.mdpi.com/1422-0067/24/11/9330 (Accessed May 27, 2023).

Ilchuk LA, Stavskaya NI, Varlamova EA, Khamidullina AI, Tatarskiy VV, Mogila VA, Kolbutova KB, Bogdan SA, Sheremetov AM, Baulin AN, et al. 2022. Limitations of Tamoxifen Application for In Vivo Genome Editing Using Cre/ERT2 System. *Int J Mol Sci* **23**. doi:10.3390/ijms232214077.

Jeyaraj DA, Grossman G, Petrusz P. 2003. Dynamics of testicular germ cell apoptosis in normal mice and transgenic mice overexpressing rat androgen-binding protein. *Reprod Biol Endocrinol* **1**: 48. doi:10.1186/1477-7827-1-48.

Ježek J, Smethurst DGJ, Stieg DC, Kiss ZAC, Hanley SE, Ganesan V, Chang K-T, Cooper KF, Strich R. 2019. Cyclin C: The Story of a Non-Cycling Cyclin. *Biology* **8**. doi:10.3390/biology8010003.

Jin F, Claessens F, Fondell JD. 2012. Regulation of androgen receptor-dependent transcription by coactivator MED1 is mediated through a newly discovered noncanonical binding motif. *J Biol Chem* **287**: 858–870. doi:10.1074/jbc.M111.304519.

Kang Z, Qiao N, Tan Z, Tang Z, Li Y. 2017. Expression patterns and changes of the LCN2 gene in the testes of induced cryptorchidism and busulfan-treated mice. *Syst Biol Reprod Med* **63**: 364–369. doi:10.1080/19396368.2017.1355416.

Kapoor A, Goldberg MS, Cumberland LK, Ratnakumar K, Segura MF, Emanuel PO, Menendez S, Vardabasso C, Leroy G, Vidal CI, et al. 2010. The histone variant macroH2A suppresses melanoma progression through regulation of CDK8. *Nature* **468**: 1105–1109. doi:10.1038/nature09590.

Korsunsky I, Fan J, Slowikowski K, Zhang F, Wei K, Baglaenko Y, Brenner M, Loh P-R, Raychaudhuri S. 2018. Fast, sensitive, and accurate integration of single cell data with

Harmony. *bioRxiv* 461954. https://www.biorxiv.org/content/10.1101/461954v2 (Accessed April 9, 2023).

Larose H, Kent T, Ma Q, Shami AN, Harerimana N, Li JZ, Hammoud SS, Handel MA. 2020. Regulation of meiotic progression by Sertoli-cell androgen signaling. *Mol Biol Cell* **31**: 2841–2862. doi:10.1091/mbc.E20-05-0334.

Lawrence MG, Lai J, Clements JA. 2010. Kallikreins on steroids: structure, function, and hormonal regulation of prostate-specific antigen and the extended kallikrein locus. *Endocr Rev* **31**: 407–446. doi:10.1210/er.2009-0034.

Li J, Hilimire TA, Liu Y, Wang L, Liang J, Gyorffy B, Sikirzhytski V, Ji H, Zhang L, Cheng C, et al. 2023. CDK19 and CDK8 Mediator kinases drive androgen-independent*in vivo*growth of castration-resistant prostate cancer. *bioRxiv*. http://biorxiv.org/lookup/doi/10.1101/2023.08.08.552491.

Liu S, Chen X, Wang Y, Li L, Wang G, Li X, Chen H, Guo J, Lin H, Lian Q-Q, et al. 2017. A role of KIT receptor signaling for proliferation and differentiation of rat stem Leydig cells in vitro. *Mol Cell Endocrinol* **444**: 1–8. doi:10.1016/j.mce.2017.01.023.

Li X, Zhu Q, Wen Z, Yuan K, Su Z, Wang Y, Zhong Y, Ge R-S. 2021. Androgen and Luteinizing Hormone Stimulate the Function of Rat Immature Leydig Cells Through Different Transcription Signals. *Front Endocrinol* **12**: 599149. doi:10.3389/fendo.2021.599149.

Martinez-Fabregas J, Wang L, Pohler E, Cozzani A, Wilmes S, Kazemian M, Mitra S, Moraga I. 2020. CDK8 Fine-Tunes IL-6 Transcriptional Activities by Limiting STAT3 Resident Time at the Gene Loci. *Cell Rep* **33**: 108545. doi:10.1016/j.celrep.2020.108545.

Ma X, Dong Y, Matzuk MM, Kumar TR. 2004. Targeted disruption of luteinizing hormone β-subunit leads to hypogonadism, defects in gonadal steroidogenesis, and infertility. *Proceedings of the National Academy of Sciences* **101**: 17294–17299. https://www.pnas.org/doi/abs/10.1073/pnas.0404743101.

McCleland ML, Soukup TM, Liu SD, Esensten JH, de Sousa e Melo F, Yaylaoglu M, Warming S, Roose-Girma M, Firestein R. 2015. Cdk8 deletion in the Apc(Min) murine tumour model represses EZH2 activity and accelerates tumourigenesis. *J Pathol* **237**: 508–519. doi:10.1002/path.4596.

Menzl I, Witalisz-Siepracka A, Sexl V. 2019a. CDK8-Novel Therapeutic Opportunities. *Pharmaceuticals* **12**. doi:10.3390/ph12020092.

Menzl I, Zhang T, Berger-Becvar A, Grausenburger R, Heller G, Prchal-Murphy M, Edlinger L, Knab VM, Uras IZ, Grundschober E, et al. 2019b. A kinase-independent role for CDK8 in BCR-ABL1+ leukemia. *Nat Commun* **10**: 4741. doi:10.1038/s41467-019-12656-x.

Missaghian E, Kempná P, Dick B, Hirsch A, Alikhani-Koupaei R, Jégou B, Mullis PE, Frey BM, Flück CE. 2009. Role of DNA methylation in the tissue-specific expression of the CYP17A1 gene for steroidogenesis in rodents. *J Endocrinol* **202**: 99–109. doi:10.1677/JOE-08-0353.

Pelish HE, Liau BB, Nitulescu II, Tangpeerachaikul A, Poss ZC, Da Silva DH, Caruso BT, Arefolov A, Fadeyi O, Christie AL, et al. 2015. Mediator kinase inhibition further activates super-enhancer-associated genes in AML. *Nature* **526**: 273–276. doi:10.1038/nature14904.

Pereira M de L, Oliveira H, Fonseca HMAC, Costa FG, Santos C. 2016. The role of cytometry for male fertility assessment in toxicology. In *Flow Cytometry - Select Topics*, InTech

http://www.intechopen.com/books/flow-cytometry-select-topics/the-role-of-cytometry-for-male-fertility-assessment-in-toxicology.

Poss ZC, Ebmeier CC, Odell AT, Tangpeerachaikul A, Lee T, Pelish HE, Shair MD, Dowell RD, Old WM, Taatjes DJ. 2016. Identification of Mediator Kinase Substrates in Human Cells using Cortistatin A and Quantitative Phosphoproteomics. *Cell Rep* **15**: 436–450. doi:10.1016/j.celrep.2016.03.030.

Postlmayr A, Dumeau CE, Wutz A. 2020. Cdk8 is required for establishment of H3K27me3 and gene repression by Xist and mouse development. *Development* **147**. doi:10.1242/dev.175141.

Povaliaeva A, Pigarova E, Zhukov A, Bogdanov V, Dzeranova L, Mel'nikova O, Pekareva E, Malysheva N, Ioutsi V, Nikankina L, et al. 2020. Evaluation of Vitamin D Metabolism in Patients with Type 1 Diabetes Mellitus in the Setting of Cholecalciferol Treatment. *Nutrients* **12**. doi:10.3390/nu12123873.

Prieto S, Dubra G, Camasses A, Aznar AB, Begon-Pescia C, Simboeck E, Pirot N, Gerbe F, Angevin L, Jay P, et al. 2023. CDK8 and CDK19 act redundantly to control the CFTR pathway in the intestinal epithelium. *EMBO Rep* **24**: e54261. doi:10.15252/embr.202154261.

Rajamanickam GD, Kastelic JP, Thundathil JC. 2017. The ubiquitous isoform of Na/K-ATPase (ATP1A1) regulates junctional proteins, connexin 43 and claudin 11 via Src-EGFR-ERK1/2-CREB pathway in rat Sertoli cells. *Biol Reprod* **96**: 456–468. doi:10.1095/biolreprod.116.141267.

Richter WF, Nayak S, Iwasa J, Taatjes DJ. 2022. The Mediator complex as a master regulator of transcription by RNA polymerase II. *Nat Rev Mol Cell Biol* **23**: 732–749. doi:10.1038/s41580-022-00498-3.

Russo JW, Nouri M, Balk SP. 2019. Androgen Receptor Interaction with Mediator Complex Is Enhanced in Castration-Resistant Prostate Cancer by CDK7 Phosphorylation of MED1. *Cancer Discov* **9**: 1490–1492. doi:10.1158/2159-8290.CD-19-1028.

Show MD, Anway MD, Folmer JS, Zirkin BR. 2003. Reduced intratesticular testosterone concentration alters the polymerization state of the Sertoli cell intermediate filament cytoskeleton by degradation of vimentin. *Endocrinology* **144**: 5530–5536. doi:10.1210/en.2003-0735.

Song W-C. 2007. The Role of Estrogen Sulfotransferase in Leydig Cells. In *The Leydig Cell in Health and Disease* (eds. A.H. Payne and M.P. Hardy), pp. 197–205, Humana Press, Totowa, NJ https://doi.org/10.1007/978-1-59745-453-7_14.

Song Z, Xiaoli AM, Li Y, Siqin G, Wu T, Strich R, Pessin JE, Yang F. 2022. The conserved Mediator subunit cyclin C (CCNC) is required for brown adipocyte development and lipid accumulation. *Mol Metab* **64**: 101548. doi:10.1016/j.molmet.2022.101548.

Sridharan S, Simon L, Meling DD, Cyr DG, Gutstein DE, Fishman GI, Guillou F, Cooke PS. 2007. Proliferation of adult sertoli cells following conditional knockout of the Gap junctional protein GJA1 (connexin 43) in mice. *Biol Reprod* **76**: 804–812. doi:10.1095/biolreprod.106.059212.

Stanton PG, Sluka P, Foo CFH, Stephens AN, Smith AI, McLachlan RI, O'Donnell L. 2012. Proteomic changes in rat spermatogenesis in response to in vivo androgen manipulation; impact on meiotic cells. *PLoS One* **7**: e41718. doi:10.1371/journal.pone.0041718.

Steinparzer I, Sedlyarov V, Rubin JD, Eislmayr K, Galbraith MD, Levandowski CB, Vcelkova T, Sneezum L, Wascher F, Amman F, et al. 2019. Transcriptional Responses to IFN-γ Require Mediator Kinase-Dependent Pause Release and Mechanistically Distinct CDK8 and CDK19 Functions. *Mol Cell* **76**: 485–499.e8. doi:10.1016/j.molcel.2019.07.034.

Stoffel W, Holz B, Jenke B, Binczek E, Günter RH, Kiss C, Karakesisoglou I, Thevis M, Weber A-A, Arnhold S, et al. 2008. Delta6-desaturase (FADS2) deficiency unveils the role of omega3- and omega6-polyunsaturated fatty acids. *EMBO J* **27**: 2281–2292. doi:10.1038/emboj.2008.156.

Stroud CK, Nara TY, Roqueta-Rivera M, Radlowski EC, Lawrence P, Zhang Y, Cho BH, Segre M, Hess RA, Brenna JT, et al. 2009. Disruption of FADS2 gene in mice impairs male reproduction and causes dermal and intestinal ulceration. *J Lipid Res* **50**: 1870–1880. doi:10.1194/jlr.M900039-JLR200.

Suzuki T. 2023. Overview of single-cell RNA sequencing analysis and its application to spermatogenesis research. *Reprod Med Biol* **22**: e12502. doi:10.1002/rmb2.12502.

Wang J-M, Li Z-F, Yang W-X. 2022. What Does Androgen Receptor Signaling Pathway in Sertoli Cells During Normal Spermatogenesis Tell Us? *Front Endocrinol* **13**: 838858. doi:10.3389/fendo.2022.838858.

Weber H, Ruoff R, Garabedian MJ. 2021. MED19 alters AR occupancy and gene expression in prostate cancer cells, driving MAOA expression and growth under low androgen. *PLoS Genet* **17**: e1008540. doi:10.1371/journal.pgen.1008540.

Welsh M, Saunders PTK, Atanassova N, Sharpe RM, Smith LB. 2009. Androgen action via testicular peritubular myoid cells is essential for male fertility. *FASEB J* **23**: 4218–4230. doi:10.1096/fj.09-138347.

Westerling T, Kuuluvainen E, Mäkelä TP. 2007. Cdk8 is essential for preimplantation mouse development. *Mol Cell Biol* **27**: 6177–6182. doi:10.1128/MCB.01302-06.

Willems A, Batlouni SR, Esnal A, Swinnen JV, Saunders PTK, Sharpe RM, França LR, De Gendt K, Verhoeven G. 2010. Selective ablation of the androgen receptor in mouse sertoli cells affects sertoli cell maturation, barrier formation and cytoskeletal development. *PLoS One* **5**: e14168. doi:10.1371/journal.pone.0014168.

Willems A, De Gendt K, Deboel L, Swinnen JV, Verhoeven G. 2011. The development of an inducible androgen receptor knockout model in mouse to study the postmeiotic effects of androgens on germ cell development. *Spermatogenesis* **1**: 341–353. doi:10.4161/spmg.1.4.18740.

Wolock SL, Lopez R, Klein AM. 2019. Scrublet: Computational Identification of Cell Doublets in Single-Cell Transcriptomic Data. *Cell Syst* **8**: 281–291.e9. doi:10.1016/j.cels.2018.11.005.

Wong EWP, Cheng CY. 2009. Polarity proteins and cell-cell interactions in the testis. *Int Rev Cell Mol Biol* **278**: 309–353. doi:10.1016/S1937-6448(09)78007-4.

Yamada T, Fukasawa K, Horie T, Kadota T, Lyu J, Tokumura K, Ochiai S, Iwahashi S, Suzuki A, Park G, et al. 2022. The role of CDK8 in mesenchymal stem cells in controlling osteoclastogenesis and bone homeostasis. *Stem Cell Reports* **17**: 1576–1588. doi:10.1016/j.stemcr.2022.06.001.

Yanai S, Baba T, Inui K, Miyabayashi K, Han S, Inoue M, Takahashi F, Kanai Y, Ohkawa Y, Choi MH, et al. 2021. Gene expression and functional abnormalities in XX/Sry Leydig cells. *Sci Rep* **11**: 719. doi:10.1038/s41598-020-80741-z.

Yang S, Corbett SE, Koga Y, Wang Z, Johnson WE, Yajima M, Campbell JD. 2020. Decontamination of ambient RNA in single-cell RNA-seq with DecontX. *Genome Biol* **21**: 57. doi:10.1186/s13059-020-1950-6.

Ye L, Li X, Li L, Chen H, Ge R-S. 2017. Insights into the Development of the Adult Leydig Cell Lineage from Stem Leydig Cells. *Front Physiol* **8**: 430. doi:10.3389/fphys.2017.00430.

Zhai G, Shu T, Yu G, Tang H, Shi C, Jia J, Lou Q, Dai X, Jin X, He J, et al. 2022. Augmentation of progestin signaling rescues testis organization and spermatogenesis in zebrafish with the depletion of androgen signaling. *Elife* **11**. doi:10.7554/eLife.66118.

Zhang S, O'Regan R, Xu W. 2020. The emerging role of mediator complex subunit 12 in tumorigenesis and response to chemotherapeutics. *Cancer* **126**: 939–948. doi:10.1002/cncr.32672.

Zhang Z, Lu Y, Qi Y, Xu Y, Wang S, Chen F, Shen M, Chen M, Chen N, Yang L, et al. 2022. CDK19 regulates the proliferation of hematopoietic stem cells and acute myeloid leukemia cells by suppressing p53-mediated transcription of p21. *Leukemia* **36**: 956–969. doi:10.1038/s41375-022-01512-5.

Zheng GXY, Terry JM, Belgrader P, Ryvkin P, Bent ZW, Wilson R, Ziraldo SB, Wheeler TD, McDermott GP, Zhu J, et al. 2017. Massively parallel digital transcriptional profiling of single cells. *Nat Commun* **8**: 14049. doi:10.1038/ncomms14049.

pagoda2: R package for analyzing and interactively exploring large-scale single-cell RNA-seq datasets. Github https://github.com/kharchenkolab/pagoda2 (Accessed May 26, 2023).